Title

Stress-induced depressive-like behavior in male rats is associated with microglial activation and inflammation dysregulation in the hippocampus in adulthood

Authors

João Paulo Brás[1,2,3], Isabelle Guillot de Suduiraut[3], Olivia Zanoletti[3], Silvia Monari[3], Mandy Meijer[3,4], Jocelyn Grosse[3], Mário Adolfo Barbosa[1,2], Susana Gomes Santos[1], Carmen Sandi[3], Maria Inês Almeida[1,2,#]

Affiliations

[1] Instituto de Investigação e Inovação em Saúde/Instituto de Engenharia Biomédica (i3S/INEB), University of Porto (UP), Rua Alfredo Allen 208, 4200-135 Porto, Portugal

[2] Instituto de Ciências Biomédicas Abel Salazar (ICBAS), University of Porto (UP), Rua de Jorge Viterbo Ferreira 228, 4050-313 Porto, Portugal

[3] Brain Mind Institute, École Polytechnique Fédérale de Lausanne (EPFL), Station 19, CH-1015 Lausanne, Switzerland

[4] Department of Human Genetics, Donders Institute for Brain, Cognition and Behaviour, Radboud University Medical Center, Nijmegen, Netherlands.

Corresponding author: ines.almeida@i3s.up.pt

Highlights

- PPS induces protracted depressive-like behaviors in H-CSR male rats.
- H-CSR PPS rats have increased hippocampal TNF-α and microglia activation.
- miR-342 is upregulated in the hippocampus of H-CSR PPS rats.
- miR-342 expression positively correlates with TNF-α and microglial activation.
- Depressive-like behaviors are associated with increased miR-342 expression.

Abstract

Neuroinflammation is increasingly recognized as playing a critical role in depression. Early-life stress exposure and constitutive differences in glucocorticoid responsiveness to stressors are two key risk factors for depression, but their impacts on the inflammatory status of the brain is still uncertain. Moreover, there is a need to identify specific molecules involved in these processes with the potential to be used as alternative therapeutic targets in inflammation-related depression. Here, we studied how peripubertal stress (PPS) combined with differential corticosterone (CORT)-stress responsiveness (CSR) influences depressive-like behaviors and brain inflammatory markers in male rats in adulthood, and how these alterations relate to microglia activation and miR-342 expression. High-CORT stress-responsive (H-CSR) male rats that underwent PPS exhibited increased anhedonia and passive coping responses in adulthood. Also, animals exposed to PPS showed increased hippocampal TNF-α expression, which positively correlated with passive coping responses. In addition, PPS caused long-term effects on hippocampal microglia, particularly in H-CSR rats, with increased hippocampal IBA-1 expression and morphological alterations compatible with a higher degree of activation. H-CSR animals also showed upregulation of hippocampal miR-342, a mediator of TNF-α-

driven microglial activation, and its expression was positively correlated with TNF-α expression, microglial activation and passive coping responses. Our findings indicate that individuals with constitutive H-CSR are particularly sensitive to developing protracted depression-like behaviors following PPS exposure. In addition, they show neuro-immunological alterations in adulthood, such as increased hippocampal TNF-α expression, microglial activation and miR-342 expression. Our work highlights miR-342 as a potential therapeutic target in inflammation-related depression.

Keywords: Peripubertal stress, corticosterone, neuroinflammation, cytokines, microRNAs

1. Introduction

The immune system is emerging as a key player in depression symptomatology and treatment resistance (1-3). A segment of depression patients present with hyperactivation of the immune system (4), including increased levels of systemic and brain proinflammatory mediators, such as TNF-α, IL-6 and IL-1β (5-9); trafficking of immune cells to the brain; and activation of microglia (10, 11). Specifically, increased levels of TNF-α have been shown to impact neurocircuits and cause neuronal damage directly, and indirectly, by overstimulating astrocytes and microglia (12, 13). Activated microglia are characterized by the of release cytotoxic molecules, including TNF-α, produced by positive feedback of autocrine activation (14, 15). The mechanisms underlying the dysregulation of the immune system in depression-like behaviors have been studied in rodents, particularly using peripheral administration of lipopolysaccharide (LPS) (16). However, from a translational perspective, it is not clear whether and how well the behavioral effects of LPS injection and the magnitude of the resulting inflammatory response “translate” to the clinic and compare to human depression (17). Therefore, the use of alternative animal models focusing on risk factors that naturally increase the susceptibility to depression development is warranted, rather than models established by exacerbated induction of systemic and local inflammation.

Risk factors for depression include early-life stress exposure and constitutive differences in glucocorticoid responsiveness to stressors (18, 19). Over the last decade, the impacts of these factors in the context of inflammation-related depression have received increasing attention (20, 21). The peripubertal period, comprising childhood and adolescence, is a critical time window in brain development that is sensitive to the deleterious effects of adverse experiences. An enhanced risk of

developing depression in adulthood following stress exposure in early life has been reported in several studies (22, 23). In our laboratory, we have shown that peripubertal stress (PPS) in rats leads to enhanced anxiety-related behaviors and increased passive stress coping responses, a key symptom in depression (18, 24). Recent findings have shown that repeated social defeat stress in adulthood leads to increased neuroinflammation and microglial activation in rats (25). However, little is known about the long-term effect of early-life stressful events on the brain inflammatory status in adulthood.

Glucocorticoids coordinate responses that enable an individual to cope with stressful challenges, mediating adaptation following a stressor's cessation (26). However, there is substantial individual variability in the magnitude of glucocorticoid responsiveness to stressors, a trait highly related to differences in coping styles (19). Recently, the view that glucocorticoids are universally anti-inflammatory has been questioned (27, 28). Persistent activation of the hypothalamus-pituitary-adrenal (HPA) axis was shown to lead to downregulation of glucocorticoid receptors involved in the negative feedback controlling the HPA axis (29). This downregulation has been associated with a failure to suppress inflammatory responses (30). We previously established a selective breeding protocol that generates lines of rats enriched for different levels of corticosterone (CORT)-stress responsiveness (CSR) (19). However, it is not known whether early-life stress differentially affects individuals who show differences in glucocorticoid stress responsiveness, in terms of protracted inflammatory marker expression and microglial activation in the brain, nor are potential correlations with indexes of depression clear. Uncovering the regulatory mechanisms governing these processes can provide new targets for the development of alternative therapeutic strategies.

In this context, microRNAs (miRNAs), which are small noncoding RNAs (approximately 20 nucleotides long) that control the expression of multiple protein targets (31), have been implicated in several mechanisms of neural plasticity, neurogenesis, stress, antidepressant treatment response and neuroinflammation (32-34), providing strong evidence that miRNAs not only can play critical roles in depression pathogenesis but are also potential therapeutic tools. Recently, we reported that miR-342 is a crucial player in TNF-α-mediated microglial activation (35). miR-342 is upregulated in TNF-α-activated microglia, and its overexpression activates, *per se*, the NF-kB pathway, leading to increased secretion of TNF-α and IL-1β, which drastically affects neuron viability (35). However, it remains to be determined how depression-like behaviors correlate with the expression levels of miR-342, particularly in the brain.

The aim of the study was to investigate how PPS and different CORT adaptations to stress impact depressive-like behaviors, inflammatory markers across different brain regions, microglial activation and miR-342 expression in adulthood. We showed that animals with high-CSR that underwent PPS exhibited increased hippocampal microglial activation and depressive-like behaviors in adulthood, which were associated with dysregulated expression of inflammatory markers, including miR-342, in the hippocampus.

2. Materials and methods

2.1. Animals

Subjects were the offspring of Wistar Han rats (Charles River Laboratories, France) bred in the animal facility of the EPFL/SV CGP *(Centre de PhénoGenómique)*. Male rats were maintained under standard housing conditions on a 12-h light-dark cycle

(lights on at 7:00 am). Food and water were available ad libitum. Animal care procedures were conducted in accordance with the Swiss Federal Guidelines for Animal Experimentation and were approved by the Cantonal Veterinary Office Committee for Animal Experimentation (Vaud, Switzerland).

2.2. Experimental design

Selective breeding of rats according to their individual differences in CSR was performed as previously described by Walker *et al.* (19). This resulted in litters (generation F14) of N-CSR (inter-line) and H-CSR (high-line). At weaning i.e., postnatal day 21 (P 21), male rats from both groups were randomly assigned to control (CTR) and PPS conditions. Animals were distributed into home cages in groups of three non-siblings. Between P 28 and P 42, animals were maintained in control conditions (CTR group) or subjected to the PPS protocol (PPS group) (Figure 1A). In adulthood (P 90), CTR and PPS rats underwent five sequential behavioral tests for anxiety (elevated plus-maze and open field/novel object), sociability (social preference), and depressive-like behavior (saccharin preference and forced-swim test) with at least 3 days of interval between each test (Figure 1A). All behavior tests were performed in the morning. In total, 42 animals were used, namely 18 N-CSR (9 CTR and 9 PPS) and 24 H-CSR (12 CTR and 12 PPS). The experimenter was blind during both testing and analysis.

2.3. Peripubertal stress

The PPS protocol was based on exposure to fear-induction procedures, according to Marquez *et al.* (24). The stressors were applied during the peripubertal period (a total of 7 days across P 28 to P 42) during the light phase and followed a variable schedule. Animals in the same cage were always assigned to the same experimental

group (either CTR or PPS). Briefly, following exposure to an open-field for 5 min on P 28, the stress protocol consisted of presenting two different fear-inducing stressors, each one lasting for 25 min. Animals were either exposed to the synthetic fox odor 2,4,5-Trimethylthiazole (TMT, Sigma-Aldrich, St. Louis, MO, USA) administered in a plastic box (38 × 27.5 × 31 cm) or to an elevated platform (EP) (12 × 12 cm) under bright light, presented alone or in combination. To assess the effect of stress exposure on the HPA axis activity, blood samples from PPS animals were collected by tail-nick (100–150 µl) at P 28, P 30, and P 42. The sampling was done immediately after stress offset and then 30 min after the first blood sampling. During this interval, rats were placed in a novel cage and were prevented of direct physical contact with their cage mates. After the second blood sampling, animals were placed back in their home cage. Control animals underwent brief handling on stress days, no blood samples were taken to minimize stress.

2.4. Evaluation of corticosterone levels

Blood samples were collected into ice-cold lithium heparin-coated capillary tubes (Sarstedt, Nümbrecht, Germany) and chilled on ice until centrifugation for plasma collection (10,000 rpm at 4°C for 4 min). Plasma was collected into new tubes and stored at −20ºC until subsequent analysis. CORT was measured in the plasma samples using an enzymatic immunoassay kit, performed according to manufacturer's instructions (Enzo Life Sciences, Farmingdale, NY, USA). Levels were calculated using a standard curve method.

2.5. Behavioral testing

2.5.1. Elevated plus maze

In adulthood, anxiety-like behavior was evaluated using the elevated plus-maze (EPM) test. The apparatus consisted of two opposing open arms (50-10 cm) perpendicular to two enclosed arms (50-10-50 cm) extending from a central platform (10-10 cm) and elevated 65 cm above the floor. Light levels were maintained at 14–16 lx on the open arms and 5–7 lx on the closed arms. At the start of the test, rats were placed in the center of the platform facing a closed arm and allowed to explore the maze for 5 min. Between animals, the apparatus was cleaned with a 5% ethanol solution and dried. Behavior was monitored using a ceiling-mounted video camera and analyzed with the computerized tracking system EthoVision 11 (Noldus IT). The time spent in the open and closed arms and the distance moved were recorded.

2.5.2. Open field/Novel object

Anxiety-related behavior was tested in the open-field (OF) and novel object (NO) test, as previously described (36). The OF and NO tests consisted of land-based tasks performed in a near-dark arena with a diameter of 1 m and a depth of 40 cm. The floor of the arena was divided into three zones: the outer zone with a diameter of 1 m, the inner zone with a diameter of 75 cm, and the center zone with a diameter of 25 cm. The light was adjusted to a level of 7 lx in the center of the arena. Animals were placed close to the wall of the arena, and OF activity was tested for a 10 min period. Subsequently, a NO (a 0.5 mL opaque green filled bottle) introduced into the center of the arena, and rat behavior was observed during the following 5 min. The activity and behavior during the whole session were recorded with a video camera, and the time spent in each of the zones (wall, intermediate zone, and center) was automatically registered and analyzed with the computerized tracking system EthoVision 11.

2.5.3. Social preference test

The social preference test (SocPT) was performed as previously described (24). Briefly, the test was performed in a rectangular, three-chambered box that included a central compartment and two side compartments. After 5 min of habituation to the central chamber, retractable doors were removed, and the rat was allowed to freely explore the whole apparatus for 10 min. The side compartments were equipped with a central, floor-fixed, transparent, perforated cylinder that contained either an unfamiliar juvenile male rat (25 ± 2 days old) or an object. The apparatus was cleaned with a 5% ethanol solution and dried between trials. The percentage of time spent exploring either the juvenile or the object was scored using Observer X11 software (Noldus IT, Wageningen, The Netherlands).

2.5.4. Saccharin preference test

Behavioral anhedonia was evaluated using the saccharin preference test (SacPT). Experimental and control groups were tested at the same time. Prior to the test, rats were single-housed and received two days of habituation to the new cage and bottle configuration (two bottles filled with tap water placed in the home cage for 24 h). A two-bottle choice procedure was used to determine baseline saccharin intake. During the test, single-housed rats were presented with two bottles (water and a 0.03% saccharin solution) in their home cage for a period of 72 h. The difference in bottle weight was determined (intake) every 24 h, and the bottle locations were counterbalanced. Saccharin preference was calculated as saccharin intake per total fluid intake (water + saccharin).

2.5.5. Forced-swim test

Rats were submitted to a forced-swim test (FST) to evaluate depression-like behavior, following previously described conditions (24). Animals were placed in a

plastic beaker (25-cm diameter x 46 cm) containing 30 cm of water (23-25°C) for 15 min. A second session was performed 24 h later for 5 min. Both sessions were recorded using video cameras mounted in front of the beakers, and the time spent immobile, swimming or diving was quantified manually in a blinded manner using Observer X11 software.

2.6. RNA extraction

After rats were sacrificed by decapitation, the brain was rapidly removed, and the hemispheres were divided. Left hemispheres were freshly dissected for isolation of the medial prefrontal cortex (mPFC), nucleus accumbens (NAc), amygdala (Amg) and hippocampus (HPC). Each brain region was placed in an RNAse-free cryotube, fresh frozen in liquid nitrogen, and stored at -80°C prior to RNA extraction. Total RNA was extracted from brain sections using TRIzol® reagent (Invitrogen, Waltham, MA, USA) according to the manufacturer's instructions. RNA concentration was evaluated using a NanoQuant Plate™ in a Spark® multimode microplate reader (Tecan, Männedorf, Switzerland). RNA integrity was evaluated by agarose gel electrophoresis.

2.7. Gene expression analysis

For gene expression analysis, RNA was treated with the TURBO DNA-free™ Kit (Invitrogen), and cDNA was synthesized using qScript® SuperMix (Quanta Biosciences, Beverly, MA, USA) according to the supplier's recommendations. Real-time quantitative polymerase chain reaction (qPCR) was carried out on a 7900HT Fast Real-Time PCR System with the 384-Well Block Module (Applied Biosystems, Waltham, MA, USA) using cDNA, primers (Microsynth, Balgach, Switzerland) and SYBR™ Green PCR Master Mix (Applied Biosystems™). Glyceraldehyde 3-phosphate dehydrogenase (GAPDH) and beta-actin (β-actin) were used as internal

controls. The expression of IBA-1 (a microglial marker) and the inflammation-related cytokines IL-1β, IL-6 and TNF-α was evaluated. The oligonucleotides used for qPCR experiments are shown in Table S1.

2.8. miRNA expression analysis

miR-342-3p expression was evaluated using TaqMan™ microRNA assays (Applied Biosystems™). Briefly, cDNA was synthesized using 30 ng of RNA as the template, a gene-specific stem-loop reverse transcription primer, and a TaqMan™ microRNA reverse transcription kit (Applied Biosystems™). qPCR was carried out on a CFX Real-Time PCR System with the 384-Well Block Module (Bio-Rad, Hercules, CA, USA) using cDNA, a TaqMan™ probe and SsoAdvanced™ Universal Probes Supermix (Bio-Rad). The small nuclear RNA U6 was used as a reference gene. Relative expression levels were calculated using the quantification cycle (Cq) method, according to MIQE guidelines (37).

2.9. Immunofluorescence

Right hemispheres were postfixed for 24 h in 4% PFA at 4°C, incubated for 48 h in a 30% sucrose solution at 4°C, flash frozen in isopentane and stored at -80°C before being further processed. Frozen brains were cut into 40-µm coronal sections with a cryostat (Leica, Wetzlar, Germany). Brain sections were blocked in PBS with 3% normal donkey serum (NDS, Jackson ImmunoResearch Laboratories, West Grove, PA, USA) and 0.3% Triton X-100 (Sigma-Aldrich) for 1 h at room temperature (RT) and incubated overnight at 4°C with goat anti-Iba-1 (ab5076, Abcam, Cambridge, UK) and rabbit anti-NeuN (ABN78, Merck Millipore, Burlington, MA, USA) primary antibodies (1:500) in PBS plus 1% donkey serum and 0.1% Triton X-100. Fluorophore-labeled anti-goat (1:500, AlexaFluor-568) and anti-rabbit (1:500, AlexaFluor-488) IgGs

were used as secondary antibodies, and DAPI (1:10000 in PBS) was used to stain the nuclei (10 min at RT). Finally, sections were mounted on SuperFrost Plus™ Adhesion slides (Thermo Scientific, Waltham, MA, USA) with Fluoromount-G® mounting medium (Southern Biotech, Birmingham, AL, USA).

2.10. Microglial morphological analysis

Images of three different subregions (CA1, CA3 and dentate gyrus (DG)) in the dorsal hippocampus were acquired using an upright confocal laser scanning microscope (Leica SP8) with a 40x glycerine immersion objective. The pixel size was set to 0.230 microns with a z-step of 0.5 microns. The acquired images were deconvolved using the SVI Huygens Professional (Scientific Volume Imaging B.V., Hilversum, The Netherlands) software program called via Huygens Remote Manager v3.7, which uses the “Classic Maximum Likelihood Estimation” algorithm (SNR = 5, quality change = 0.001, max. iterations = 50). Analysis of the deconvolved images was performed with Fiji (38) and Imaris (BitPlane, South Windsor, CT, USA) using the EasyXT-Fiji (https://github.com/BIOP/EasyXT-FIJI) plugin via a custom groovy script. Briefly, Imaris surfaces were created to segment the arborization of cells (smoothing=0.230, threshold=7) and for their soma (smoothing=1, threshold=10). Next, cells were created by linking each soma to its corresponding arborization based on the nearest centers of mass. Next, for each cell, the mask of the arborization was sent to Fiji, 1) skeletonized and analyzed (average and maximum branch lengths, number of branches), and 2) downsampled to calculate its 3D Convex Hull (39), which was then upscaled back to the original size. Finally, the masks of the Skeleton and 3D Convex Hull were sent back to the Imaris Scene, and a results file was created with volumes and calculated ratios. This approach was chosen to avoid possible biases induced by a z-axis maximum intensity projection used to render 3D data in 2D.

2.11. Statistical analysis

Statistical analysis was performed using GraphPad Prism version 7 (GraphPad Software, San Diego, CA, USA). Gaussian distribution was tested by the D'Agostino & Pearson and Shapiro-Wilk normality tests. When analyzing the difference between the means of more than two groups, 2-way ANOVA was performed to estimate how the mean of the quantitative variables changed according to the levels of the independent variables (CSR and stress exposure). To test which levels were actually different between the CTR and PPS groups, Sidak's post hoc multiple comparisons test was performed. Pearson correlation analysis were performed considering all animals (N=42), and the resulting r and p-values are represented in each plot. All bars and error bars represent the mean ± SEM. The sample size and the statistical tests used are indicated in each figure legend. $p<0.05$ was considered statistically significant.

3. Results

3.1. Exposure to peripubertal stress gives rise to dissociable alterations in social and depressive-like behaviors in adulthood

After weaning, animals were exposed to a PPS protocol based on fear-induction procedures between P 28 and P 42 (Figure 1A). During the PPS protocol, CORT levels were measured in plasma samples collected on P 28, P 30, and P 42. Analysis of the CORT concentration revealed a significant interaction between selection CSR groups and sampling timepoints (2-way RM ANOVA: $F_{(2,38)} = 5.937$, $p = 0.0057$, Figure 1B). In accordance with our previous data (19, 40), after the first stressor exposure (P 28), the N-CSR and H-CSR groups did not differ in their CORT response (2-way RM ANOVA post hoc test: $P\ 28_{(N\text{-}CSR\ vs\ H\text{-}CSR)}$: $t = 1.389$, $p = 0.428$) but showed significant

differences on the third (P $30_{(N\text{-}CSR\ vs\ H\text{-}CSR)}$: $t = 3.88$, $p < 0.001$) and last days of the protocol (P $42_{(N\text{-}CSR\ vs\ H\text{-}CSR)}$: $t = 4.84$, $p < 0.001$), with H-CSR rats showing increased CORT levels compared with N-CSR rats (Figure 1B).

Anxiety-like behaviors

To address the impact of different CSRs and PPS on anxiety-like behaviors in adulthood, EPM and OF/NO tests were performed (Figure 1C and D). In the EPM test, no significant interactions were found between different CSRs and PPS exposure in the time spent in the CA ($F_{(1,38)} = 0.864$, n.s.) or in the OA ($F_{(1,38)} = 0.601$, n.s.). Neither different CSRs nor PPS exposure influenced the time spent in the CA/OA (Figure 1C). Additionally, the number of entries in zone and total distance moved in the EPM test were not affected by either different CSRs or PPS exposure (Figure S1A). Generally, animals spent more time in the protected closed arms than in the open arms of the maze, independent of their CSR or stress exposure ($F_{(3,76)} = 13.69$, $p < 0.001$; Figure 1C).

In the OF test, a significant interaction was observed between different CSRs and PPS exposure in the time spent in the wall ($F_{(1,38)} = 5.465$, $p = 0.025$) and intermediate zones ($F_{(1,38)} = 9.003$, $p = 0.0248$; Figure 1D). H-CSR rats submitted to the PPS protocol spent significantly more time in the wall zone (H-CSR $_{(CTR\ vs\ PPS)}$: wall: $t = 2.351$, $p = 0.047$) and less time in the intermediate zone than those in the H-CSR non-PPS control group (H-CSR $_{(CTR\ vs\ PPS)}$: inter: $t = 3.077$, $p = 0.007$; Figure 1D). Conversely, the time spent across the different zones by N-CSR rats was not affected by PPS exposure (Figure 1D). Of note, the total distance moved during the test was not affected by either different CSRs or PPS exposure (Figure S1B). After 10 min of open-field tracking, an NO was introduced into the center of the arena, and the behavior was recorded for an extra 5 min. The introduction of the NO induced high

variability in the behavioral responses across all experimental groups, and no differences were found (Figure S1C).

Social behaviors

In the SocPT, the time spent exploring the juvenile was significantly impacted by both different CSRs ($F_{(1,38)} = 5.350$, $p = 0.026$) and PPS exposure ($F_{(1,38)} = 13.850$, $p < 0.001$; Figure 1E), although the interaction between both factors was not statistically significant ($F_{(1,38)} = 0.052$, n.s.). In fact, rats from both the N-CSR and H-CSR groups submitted to PPS interacted with the juvenile for significantly less time than the respective controls (N-CSR $_{(CTR\ vs\ PPS)}$: $t = 2.612$, $p = 0.025$; H-CSR $_{(CTR\ vs\ PPS)}$: $t = 2.669$, $p = 0.022$; Figure 1E). In addition to the influence on the time spent exploring the juvenile, PPS rats showed a reduction in total exploration (juvenile + object) ($F_{(1,38)} = 13.22$, $p < 0.001$; Figure S1D). These results show that PPS significantly decreases animals' motivation to engage in social exploration and interaction, independently of their CSR.

Depressive-like behaviors

Depressive-like behaviors were evaluated by SacPT and FST. Anhedonia evaluation in rodents takes advantage of their innate preference for sweet tastes (41). The results showed that PPS exposure significantly impacted saccharin preference on the second ($F_{(1,38)} = 5.354$, $p = 0.026$) and third days of the test ($F_{(1,38)} = 4.832$, $p = 0.034$). Post hoc analysis revealed that H-CSR rats subjected to PPS had a significantly lower preference for saccharin than the respective control non-PPS rats (H-CSR $_{(CTR\ vs\ PPS)}$: day 2: $t = 2.603$, $p = 0.025$; day 3: $t = 3.085$, $p = 0.016$; Figure 1F). On the other hand, no significant differences were found in N-CSR rats when comparing the PPS and CTR groups (Figure 1E). Importantly, total consumption (water + saccharin) did not change among the groups (Figure 1E).

The FST is widely used to assess animals' coping behaviors. We exposed rats to a two-day forced-swimming procedure and quantified the time spent immobile. During the first episode of the FST, neither CSR ($F_{(1,38)}$ = 0.6479, n.s.) nor PPS ($F_{(1,38)}$ = 0.0397, n.s.) influenced animals' behavioral response in terms of time spent floating (Figure S1F). However, during the second exposure, the time spent floating was significantly increased by PPS exposure ($F_{(1,38)}$ = 7.696, p = 0.008). Post hoc analysis revealed that H-CSR rats but not N-CSR rats (N-CSR *(CTR vs PPS)*: t = 1.449, n.s.) that underwent PPS spent significantly more time floating than H-CSR non-PPS control rats (H-CSR *(CTR vs PPS)*: t = 2.564, p = 0.028; Figure 1G). Therefore, although there is no statistical interaction between CSR and PPS, H-CSR rats seem to be more susceptible to PPS exhibiting depressive-like behaviors in adulthood.

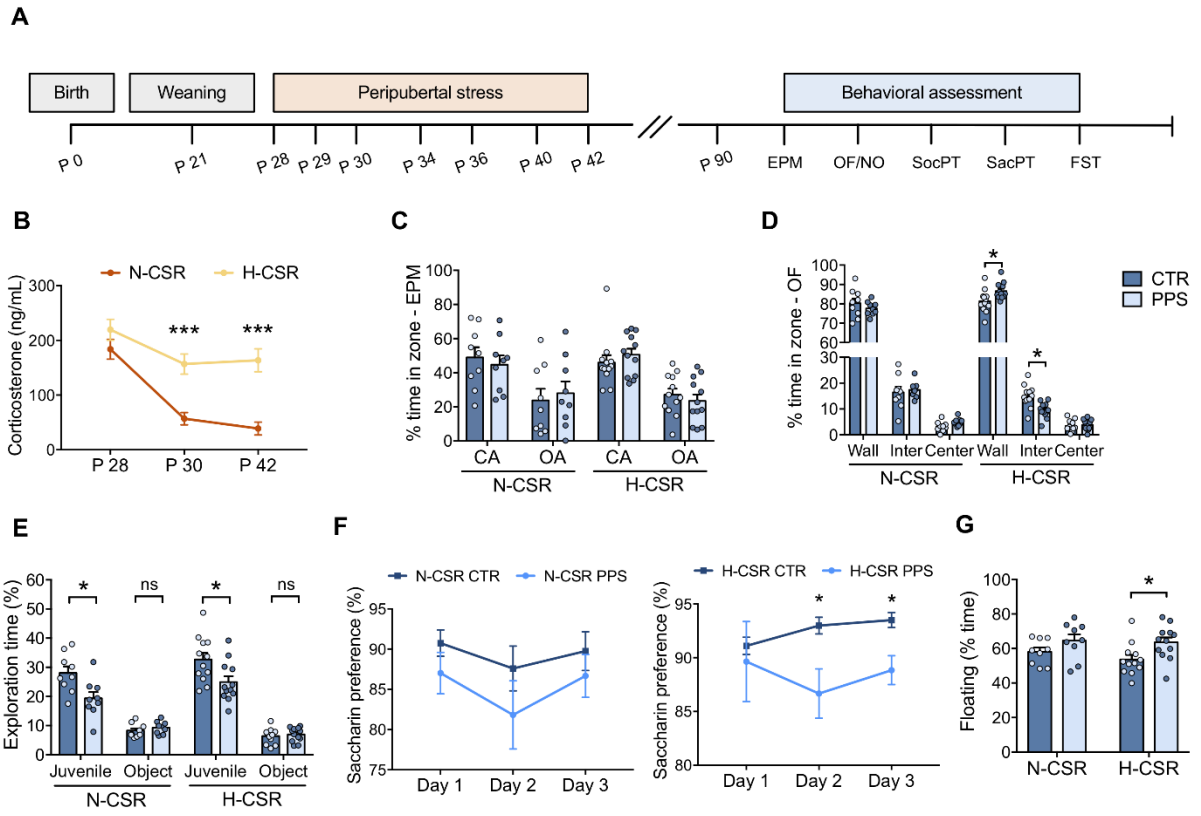

Figure 1. Effects of peripubertal stress on anxiety-like, social and depression-like behaviors in rats with differential CORT stress responsiveness in

adulthood. (A) Experimental procedures and timeline. (B) Plasma CORT levels of normative- (N-CSR) and high-CORT stress responsive (H-CSR) rats after stress exposure at P 28, P 30 and P 42. (C-G) In adulthood, animals went through a battery of tests for anxiety-like (EPM and OF), social (SocPT) and depressive-like behaviors (SacPT and FST). In the EPM (C) and OF (D) tests, the % of time spent in each zone was calculated using EthoVision 11. In SocPT (E), the % of time spent exploring either the juvenile or the object was scored using Observer X11. In the SacPT (F), single-housed rats were presented with two bottles (water and a 0.03% saccharin solution) for 72 h, and saccharin preference (%, saccharin intake/total consumption) was calculated every 24h. In the FST (G), two trials were performed, recorded and quantified manually in a blinded manner using Observer X11. The graph represents the % of time spent floating/immobile in the second trial. N: N-CSR = 18 (9 CTR and 9 PPS); H-CSR = 24 (12 CTR and 12 PPS). Results are expressed as the mean ± SEM. Two-way ANOVA followed by Sidak's post hoc multiple comparisons test, *$p < 0.05$, **$p < 0.01$, ***$p < 0.001$, n.s.: nonsignificant. CA - closed arms, OA - open arms.

3.2. Hippocampal TNF-α expression is enhanced by peripubertal stress and positively correlates with depressive-like behaviors in adulthood

Next, we evaluated the impact of PPS and different CSRs on proinflammatory markers across different brain regions known to be involved in the pathophysiology of depression. The expression levels of IL-1β, IL-6, TNF-α and IBA-1 were evaluated in the mPFC, NAc, Amg and HPC (Figure 2 and Table S2).

In the mPFC, PPS did not significantly affect any of the tested inflammatory markers (Figure 2A and Table S2). In contrast, mPFC levels of IL-1β ($F_{(1,38)} = 17.12$, $p < 0.001$), IL-6 ($F_{(1,38)} = 42.42$, $p < 0.001$) and IBA-1 ($F_{(1,38)} = 67.76$, $p < 0.001$), were

significantly increased in H-CSR rats compared with N-CSR rats, independently of PPS exposure (Table S2). In the NAc, PPS significantly impacted the levels of TNF-α ($F_{(1,38)} = 5.24$, $p = 0.0278$). In particular, H-CSR PPS rats showed increased levels of TNF-α compared with H-CSR non-PPS control rats (H-CSR $_{(CTR\ vs\ PPS)}$: TNF-α: $t = 2.730$, $p = 0.019$; Figure 2B and Table S2). Moreover, IL-1β ($F_{(1,38)} = 5.505$, $p = 0.025$), IL-6 ($F_{(1,38)} = 11.40$, $p = 0.002$) and TNF-α ($F_{(1,38)} = 5.955$, $p = 0.019$) expression was upregulated in H-CSR rats compared with N-CSR rats, independently of PPS (Table S2). In the Amg, the expression levels of the tested inflammatory markers were not affected by PPS or different CSRs (Figure 2C and Table S2). In the HPC, PPS exposure significantly impacted the expression levels of TNF-α ($F_{(1,38)} = 11.37$, $p = 0.002$) and IBA-1 ($F_{(1,38)} = 7.18$, $p = 0.011$; Figure 2D and Table S2), independently of CSR. Post hoc analysis revealed that when comparing PPS animals versus the respective control animals, IBA-1 expression was increased in H-CSR rats (H-CSR $_{(CTR\ vs\ PPS)}$: IBA-1: $t = 3.777$, $p = 0.001$), while TNF-α expression was increased in both N-CSR rats (N-CSR $_{(CTR\ vs\ PPS)}$: TNF-α: $t = 2.40$, $p = 0.042$) and H-CSR rats (H-CSR $_{(CTR\ vs\ PPS)}$: TNF-α: $t = 2.385$, $p = 0.044$; Figure 2D and Table S2).

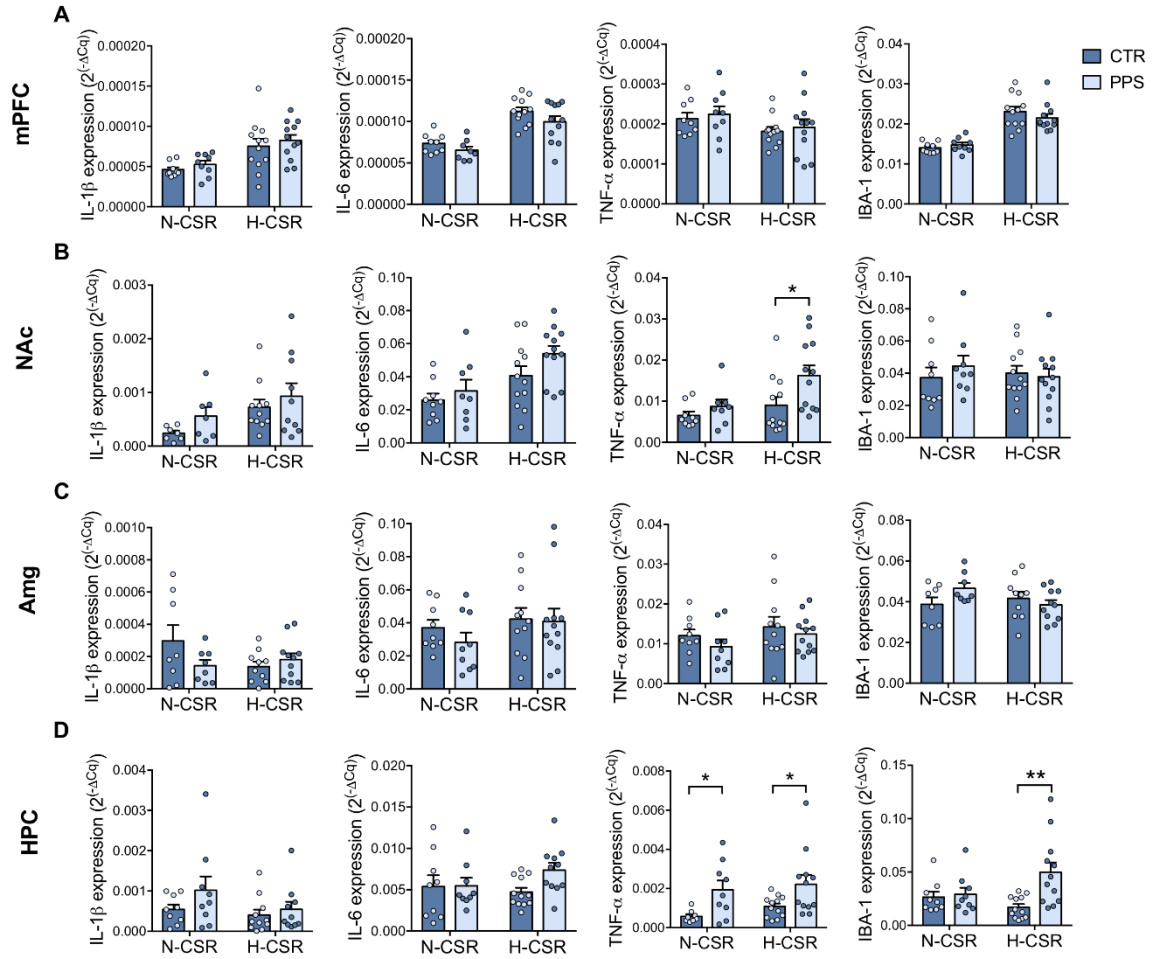

Figure 2. Expression levels of inflammatory markers across different brain regions in adulthood. The mRNA expression levels of IL-1β, IL-6, TNF-α and IBA-1 in the medial prefrontal cortex (mPFC) (A), nucleus accumbens (NAc) (B), amygdala (Amg) (C) and hippocampus (HPC) (D) were evaluated by RT-qPCR using GAPDH and β-actin as internal controls. Relative expression levels were calculated using the quantification cycle (Cq) method, according to the MIQE guidelines, and results are presented as the mean ± SEM. N-CSR = 18 (9 CTR and 9 PPS); H-CSR = 24 (12 CTR and 12 PPS); 2-way ANOVA followed by Sidak's post hoc multiple comparisons test was performed to evaluate significant differences among groups. Statistical differences between CTR and PPS animals are highlighted with asterisks *$p < 0.05$, **$p < 0.01$, ***$p < 0.001$.

To explore possible correlations between the expression levels of inflammatory molecules and depressive-like behaviors, Pearson correlation analyses were performed. No significant correlations were found between the tested inflammatory markers in the mPFC, NAc and Amg and depressive-like behaviors (Figure S2, S3 and S4). However, in the HPC, TNF-α (but not IL-1β, IL-6 or IBA-1) was positively correlated with the % of time spent floating on the second day of the FST (% time floating vs TNF-α: $r = 0.3799$, $p = 0.014$; Figure 3), suggesting that increased TNF-α expression levels in the hippocampus might contribute to or be a consequence of depressive-like behaviors.

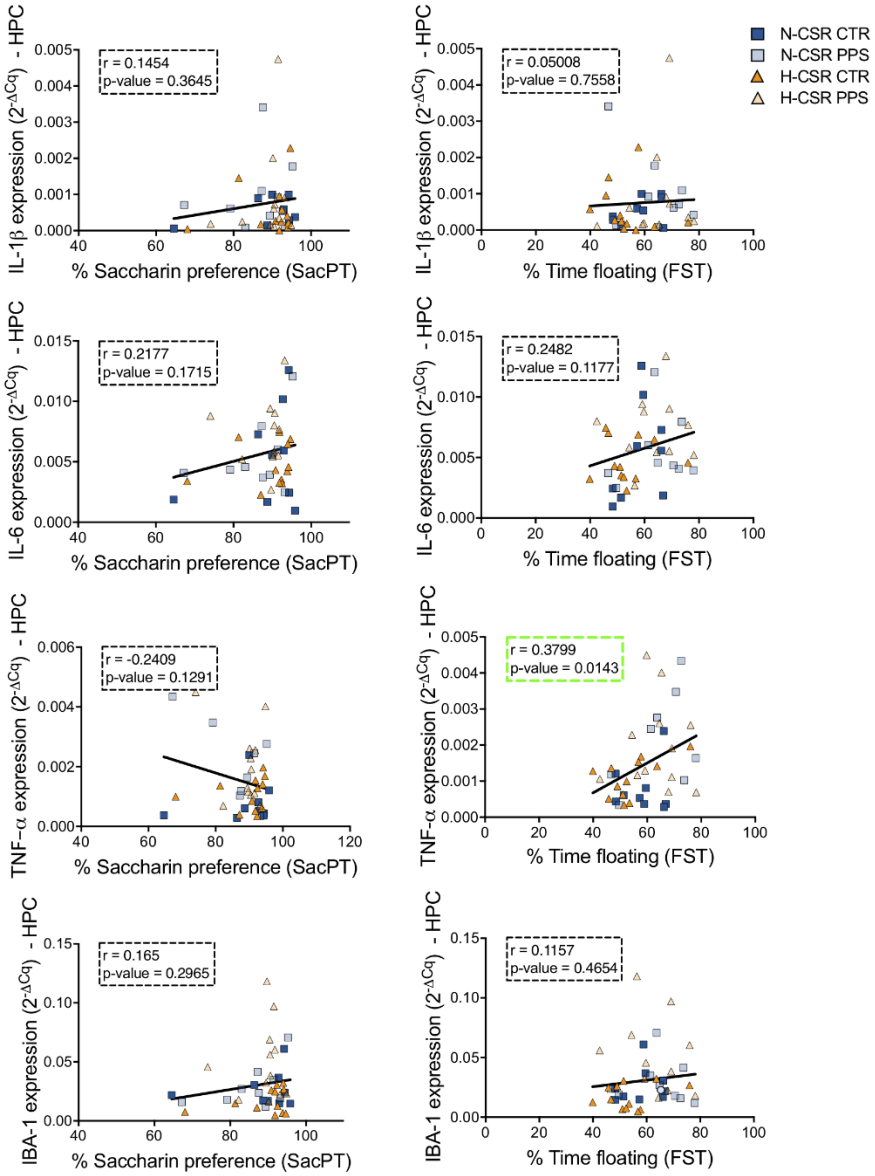

Figure 3. Correlations between the expression levels of inflammatory markers in the hippocampus and depressive-like behaviors. Pearson correlation analyses were performed by comparing the mRNA expression levels of IL-1β, IL-6, TNF-α and IBA-1 in the hippocampus and % saccharin preference (SacPT) or % of time spent floating (FST). Correlations were performed considering all animals (N=42). The

coefficient r and p-value for each correlation are presented in a box. Statistically significant correlations are highlighted in green ($p<0.05$).

3.3. Peripubertal stress induces microglial activation in the hippocampus of high-CORT stress-responsive rats

Following the detection of increases in TNF-α and IBA-1 in the HPC of adult rats that had been exposed to PPS, particularly H-CSR animals, and considering that hippocampal TNF-α levels were positively correlated with depressive-like behavior, as measured by the FST (Figure 3), we next investigated the microglial activation status. This evaluation is important for understanding whether hippocampal homeostasis is partially compromised. Typically, activated microglia exhibit an ameboid morphology with an increased soma area, a decreased arborization area and a decreased number of branches (42). Microglial morphology was evaluated by immunofluorescence staining for IBA-1 (a marker of microglial activation) in the CA1, CA3 and dentate gyrus (DG) subregions of the dorsal hippocampus, and 3D morphological analysis was performed with IMARIS software for a more robust analysis (Figure 4A, Figure S5 and S6). On average, more than 20 cells per animal were analyzed to evaluate soma volume, arborization volume, convexHull volume, average branch length, max. branch length and total number of branches (Figure 4A-C and Figure S6).

PPS induced alterations in hippocampal microglial morphology in adulthood, particularly in terms of arborization volume ($F_{(1,38)} = 7.045$, $p = 0.012$) and total number of branches ($F_{(1,38)} = 5.186$, $p = 0.029$; Figure 4B and C). Of note, a significant interaction between stress exposure and different CSRs was found in terms of the total number of branches ($F_{(1,38)} = 5.256$, $p = 0.027$). Independent of PPS, different CSRs tended to induce similar alterations in microglial morphology, although the differences did not reach statistical significance (arbo vol: $F_{(1,38)} = 3.806$, $p = 0.058$;

branch number: $F_{(1,38)}$ = 2.857, p = 0.099; Figure 4B and C). Importantly, post hoc analysis revealed that PPS H-CSR rats exhibited significant decreases in arborization volume (H-CSR$_{(CTR\ vs\ PPS)}$: t = 3.064, p = 0.008), convexHull volume (H-CSR$_{(CTR\ vs\ PPS)}$: t = 2.359, p = 0.047) and total number of branches (H-CSR$_{(CTR\ vs\ PPS)}$: t = 3.613, p = 0.002) compared with H-CSR animals in control (non-PPS) conditions, suggesting alterations in PPS H-CSR rat microglial morphology compatible with a higher degree of activation (Figure 4B and C).

Importantly, we found hippocampal IBA-1 expression levels to be negatively correlated with microglial arborization volume (arbo vol vs IBA-1: r = -0.371, p = 0.018) and with the number of branches (branch number vs IBA-1: r = -0.372, p = 0.018; Figure 4D). Moreover, although not statistically significant, hippocampal microglial arborization volume tended to be negatively correlated with the % of time spent floating on the second day of the FST (arbo vol vs % time floating: r = -0.300, p = 0.060; Figure 4E). Overall, these results show increased hippocampal microglial activation in adult H-CSR rats subjected to PPS.

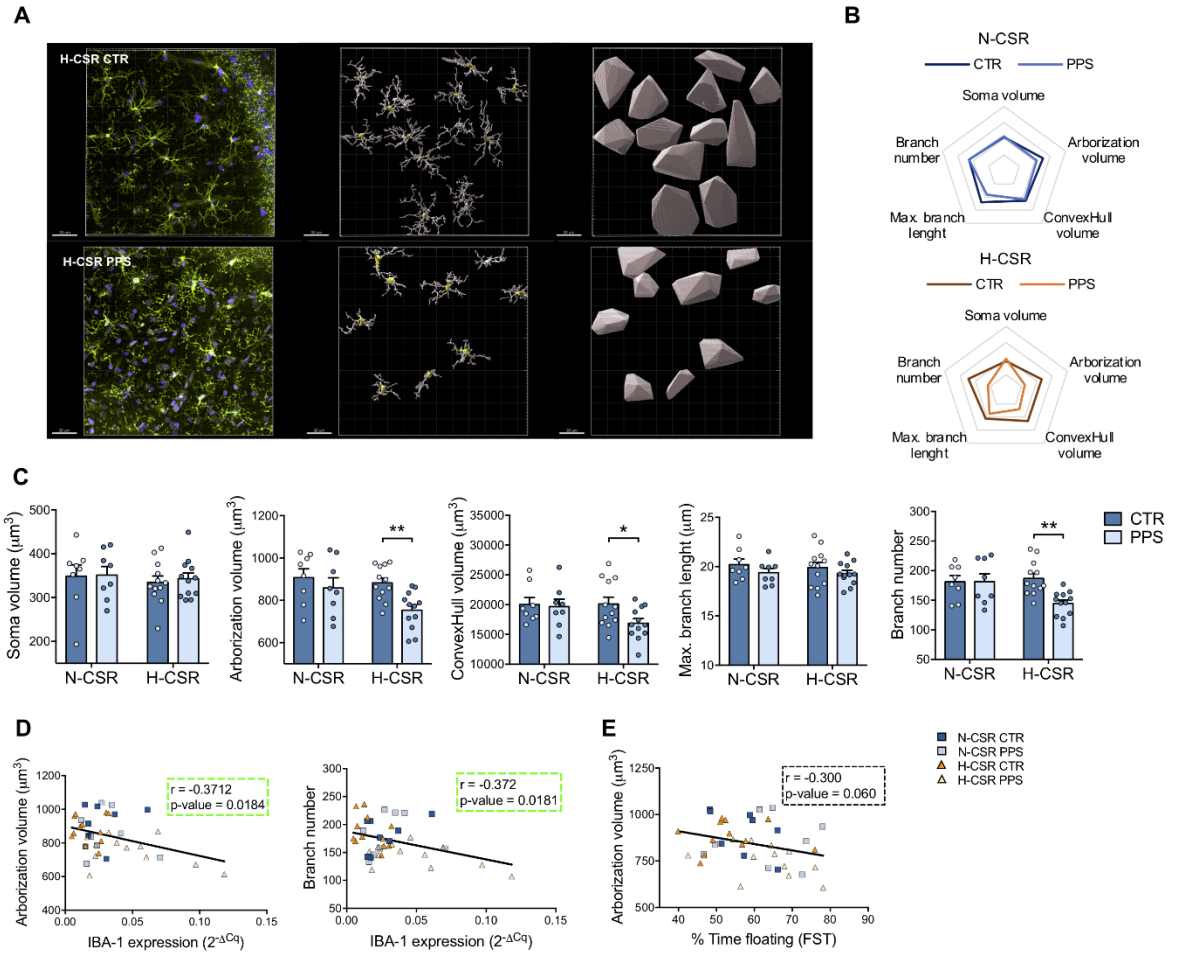

Figure 4. Morphological analysis of hippocampal microglia. To evaluate microglial activation, images of IBA-1-positive microglia in three different subregions of the dorsal hippocampus (CA1, CA3 and DG) were acquired, and microglial morphology analyzed. (A) Representative images showing IBA-1-positive microglia in the CA1 subregion in green (left). IMARIS 3D arborization (center) and IMARIS convexHull (right) visualizations of H-CSR CTR and PPS rats (scale bar: 30 µm). (B) Radar chart containing the average results of the most relevant morphological features analyzed. (C) Quantitative analysis of hippocampal microglial morphology. Results represent the average values of the 3 subregions. Each dot represents an animal (N: N-CSR = 18 (9 CTR and 9 PPS); H-CSR = 24 (12 CTR and 12 PPS)). On average, more than 20 cells per rat were analyzed for soma volume, arborization volume, convexHull volume,

max. branch length and total number of branches. Results are expressed as the mean ± SEM. Two-way ANOVA followed by Sidak's multiple comparisons test, *p < 0.05. (D-E) Pearson correlation analyses were performed by comparing significantly altered morphological features (arborization volume and total number of branches) and IBA-1 expression (D) and arborization volume and % of time spent floating (FST) (E). Correlations were performed considering all animals (N=42). The coefficient r and p-value for each correlation are presented in a box. Statistically significant correlations are highlighted in green (p<0.05).

3.4. miR-342 expression in the hippocampus is positively correlated with TNF-α expression, microglial activation and depressive-like behaviors

In addition to cytokines, inflammatory miRNAs (called inflammiRs) are crucial molecules in the regulation of microglial activation (34). This is the case for miR-342, which we previously identified as a key player in TNF-α-driven microglial activation and a potential target for tackling microglia-driven neuroinflammation (35). Considering the morphological changes in the hippocampal microglia of H-CSR adult rats following PPS, we investigated miR-342 expression in the hippocampus. miR-342 expression levels were significantly impacted by stress exposure ($F_{(1,38)}$ = 7.128, p = 0.011; Figure 5A). Post hoc analysis revealed that miR-342 expression levels were significantly increased in H-CSR rats undergoing PPS compared with the respective non-PPS control rats (H-CSR$_{(CTR\ vs\ PPS)}$: t = 2.681, p = 0.021), while no significant differences were found for the N-CSR PPS versus CTR groups (N-CSR$_{(CTR\ vs\ PPS)}$: t = 1.210, p = 0.412; Figure 5A). Interestingly, hippocampal miR-342 expression was positively correlated with TNF-α expression (miR-342 vs TNF-α: r = 0.400; p = 0.009;

Figure 5B) and negatively correlated with microglial arborization volume (miR-342 vs arbo vol: r = -0.351; p = 0.026; Figure 5C).

Subsequently, the correlation between hippocampal miR-342 expression and depressive-like behaviors revealed a significant positive correlation between miR-342 levels and the percentage of time spent floating on the second day of the FST (miR-342 vs % time floating: r = 0.479; p = 0.0013; Figure 5D) and a tendency toward a negative correlation with saccharin preference (miR-342 vs % sac pref: r = -0.288; p = 0.063; Figure 5D). These results suggest that hippocampal miR-342 expression may be a factor in microglial activation and depression susceptibility.

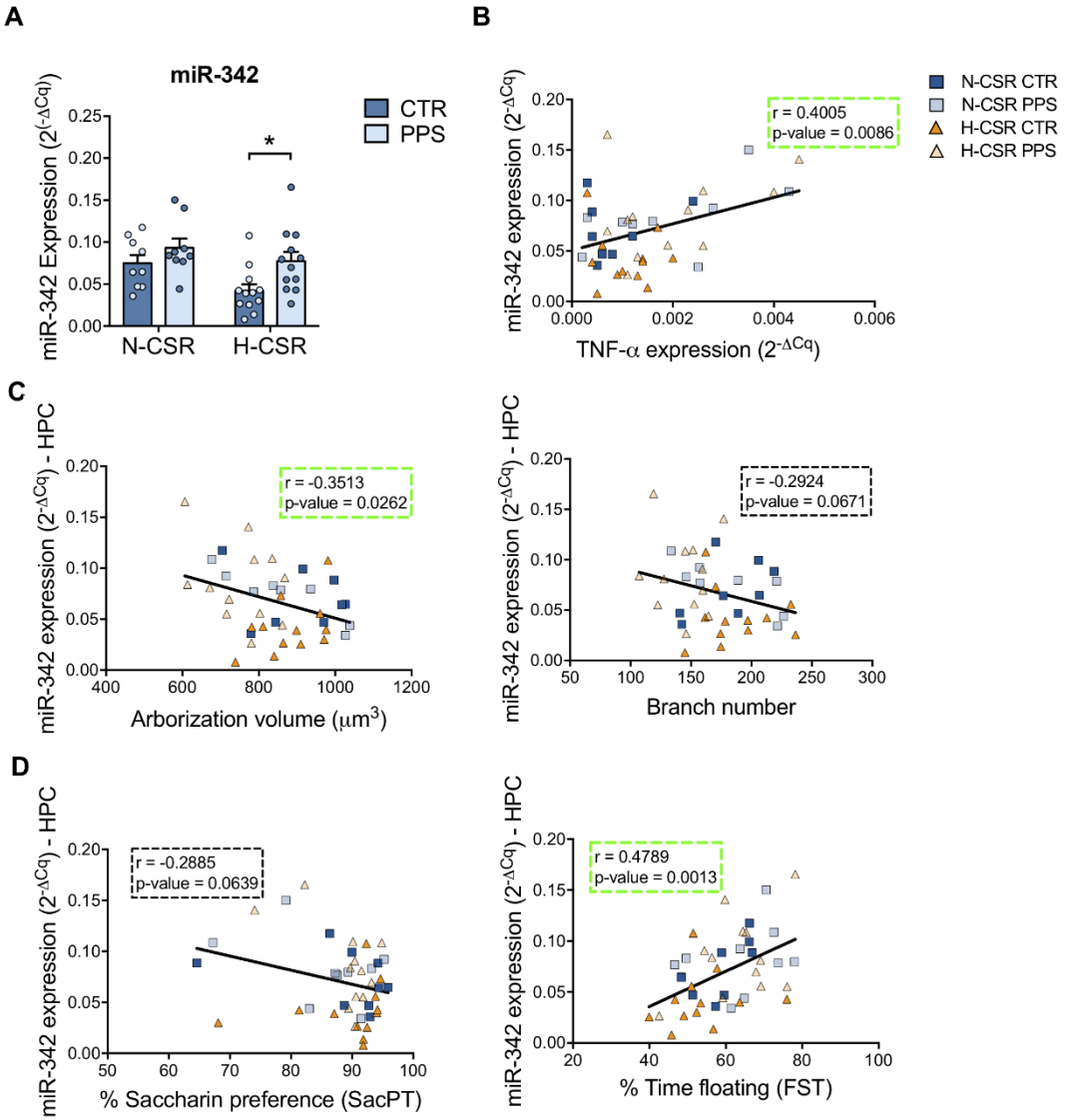

Figure 5. miR-342 expression analysis in the hippocampus. (A) miR-342 expression levels in the hippocampus were evaluated by RT-qPCR using U6 snRNA as an internal control. Relative expression levels were calculated using the quantification cycle (Cq) method, according to the MIQE guidelines, and results are presented as the mean ± SEM. N: N-CSR = 18 (9 CTR and 9 PPS); H-CSR = 24 (12 CTR and 12 PPS). Two-way ANOVA followed by Sidak's multiple comparisons test, *p < 0.05. (B-D) Pearson correlation analyses were performed to evaluate possible correlations between hippocampal miR-342 expression and TNF-α expression (B), microglial activation/altered morphological features (C) and depressive-like behaviors

(D). Correlations were performed considering all animals (N=42). The coefficient r and p-value for each correlation are presented in a box. Statistically significant correlations are highlighted in green ($p<0.05$).

4. Discussion

The “inflammation-related depression” hypothesis has been under debate, and recent findings increasingly support a link between inflammation and depression. First, it has been reported that a subgroup of depression patients exhibits increased levels of peripheral inflammatory markers (9, 43). Second, proinflammatory cytokines have been found to be elevated in the cerebrospinal fluid of a segment of depression patients (44). Third, while studies regarding the anti-inflammatory properties of traditional antidepressants are contradictory (45-48), inflammation is more aberrant in treatment nonresponders (49, 50), with significant associations between the number of failed treatment trials and increased levels of TNF-α, IL-6 and C-reactive protein (50). These findings have identified new challenges in the discovery of inflammatory mediators that can serve as biomarkers and/or alternative targets for the treatment of inflammation-related depression.

Early-life stress exposure and constitutive differences in glucocorticoid responsiveness to stressors can influence the risk of depression (51-53), but their effect on inflammatory mediators in the brain remain largely unexplored. We investigated how these two factors influence depressive-like behaviors, neuroinflammation and their neurobiological correlates. PPS alone was sufficient to induce reduced sociability in adult male rats, independent of CORT stress responsiveness. However, only those with a lower degree of adaptation of their CORT responses (H-CSR group) and undergoing PPS, exhibited increased anhedonia and

passive coping responses, when compared to their respective CSR control group. Given the fact that the behavioral responses from N-CSR PPS rats did not differ from those of N-CSR CTR animals, this suggests that increased CORT levels enhance the susceptibility of animals to late effects of stress and, consequently, the exhibition of depressive-like behaviors in adulthood. Although a chronic increase in CORT was previously reported to be sufficient to induce depression-like behaviors in rats (54), we found that H-CSR alone, without priming by stressful events, was not sufficient to induce depressive-like behaviors in male rats. Nonetheless, a limitation of this study is the use of males only, while sex-specific mechanisms have been shown to regulate response to stress and the development of depression outcomes (55). A question to address in the future is whether sex differences influence the long-term effect of PPS in terms of brain inflammatory markers.

Following our hypothesis that PPS in combination with H-CSR might contribute to increased inflammation and depression-like behaviors, we evaluated the expression of inflammatory markers across different brain regions in adulthood. We found that animals with high-CORT stress responsiveness exhibited increased levels of IL-1β, IL-6 and IBA-1 in the mPFC and IL-1β, IL-6 and TNF-α in the NAc. With the exception of TNF-α in the NAc, all these inflammatory markers were altered independently of PPS, suggesting that their levels in these regions may not be associated with depressive-like behaviors but rather with CORT regulation. In contrast, TNF-α expression in the NAc was increased in high-CSR rats that underwent PPS (i.e., rats exhibiting depressive-like behaviors). However, these levels in the NAc were not statistically correlated with either the % of saccharin preference or % of floating time in the FST. Interestingly, TNF-α expression was also increased in the hippocampus of both N-CSR and H-CSR rats submitted to PPS, and most importantly, hippocampal

TNF-α expression was positively correlated with the worsening of depressive-like behaviors (as shown by FST). In fact, several clinical trials have provided evidence on the efficacy of different anti-TNF-α drugs in depressive symptoms/disorder (56). Monoclonal antibody drugs against TNF-α, such as infliximab and adalimumab, were shown to be effective in improving mood in treatment-resistant depression patients (57), as well as in Chron's disease and psoriasis patients (58, 59). On the other hand, etanercept, a TNF-α receptor blocker, was also shown to reduce secondary depressive symptoms to some extent in patients suffering from psoriasis (60, 61).

Despite having an important role in brain development (62), a chronic increase in TNF-α levels is known to have deleterious effects on brain cells and neurocircuits. First, TNF-α is known to induce indoleamine 2,3 dioxygenase (IDO)-mediated tryptophan degradation through the kynurenine pathway, which generates neuroactive metabolites, including kynurenic acid and quinolinic acid, ultimately influencing serotonergic neurotransmission (63). Second, TNF-α can potentiate glutamate-mediated excitoneurotoxicity indirectly by inhibiting glutamate transport on astrocytes and directly by stimulating extensive microglial and/or astrocyte glutamate release in an autocrine manner (12, 13, 64). Indeed, in response to their dynamic surrounding environment, microglia display a remarkable degree of phenotypic plasticity, in terms of both morphology and molecular markers (65). While microglial reactivity may initially contribute to the restoration of tissue homeostasis, persistent inflammation that overstimulates microglia leads to a sequence of events that compromise neuronal survival (66).

In fact, we found that PPS produced late effects on hippocampal microglia, particularly in animals with high-CSR (i.e., animals exhibiting depressive-like behaviors), with increased hippocampal IBA-1 expression and morphological

alterations compatible with a higher degree of activation. In line with our findings, Gong *et al.* reported that early social isolation in mice induced depressive-like behaviors and loss and dystrophy of hippocampal microglia in adulthood, caused by increased activation of these cells (67). Nonetheless, since separate hemispheres were used to perform gene expression and microglia morphological analysis, we do not exclude any laterality effect. Additionally, it is possible that the dysregulation of microglial activation and cytokine expression levels may also be occurring in other brain regions, as described by others (68). However, according to the expression levels of the inflammatory markers tested over distinct brain regions, alterations in TNF-α and IBA-1 expression were more evident in the hippocampus. In agreement, multiple reports focusing on the late effects of early-life stress in terms of depressive-like behaviors highlight major alterations in the hippocampus compared with other regions of the brain (69).

Identifying specific molecules underlying cytokine expression, microglial dysregulation and depression symptoms is of interest for the development of novel targeted therapeutic drugs. Since the first demonstration of their involvement in human diseases in 2002 (70), miRNAs have emerged as therapeutic targets in distinct pathologies due to their capacity to regulate protein levels, including those of inflammatory markers, and influence the course of disease, patient response to treatment and clinical outcome (71). However, few studies have referred to the late effects of early-life stress on depression and miRNA expression. Among studied miRNAs, miR-124a and miR-18a were shown to be upregulated in the PFC and HPC in adulthood and were associated with depressive-like behaviors (72), while miR-146a overexpression was shown to improve depressive-like behaviors in mice by inhibiting microglial activation (73) and to protect against cognitive decline-induced surgical

trauma by suppressing hippocampal neuroinflammation (74). In a previous *in vitro* study, we identified miR-342 as a potential target for resolving neuroinflammation (35). In particular, miR-342 was found to be upregulated in microglia primed with TNF-α, and its overexpression was shown to activate the NF-kB pathway, leading to increased secretion of TNF-α, IL-1β and nitrites and drastically affecting neuron viability (35). Herein, we associated hippocampal miR-342 expression with depressive-like behaviors for the first time. Strikingly, we found hippocampal miR-342 to be positively correlated with TNF-α expression and microglial activation. These results not only support the previously established hypothesis of strong interplay between miR-342 and TNF-α in potentiating microglial activation but also identify miR-342 as a novel potential therapeutic target for microglial activation in the hippocampus and for inflammation-related depression. Moreover, since inflammatory mediators in the hippocampus were specifically correlated with forced swim performance, an alternative line of research is to address is how hippocampal TNF-α, microglia and miR-342 mediate the programming effects of PPS on memory performance in adulthood (75).

Of note, preclinical studies in Alzheimer's disease (AD) and Parkinson's disease (PD) using miR-342-3p antagomir and anti-miR-342-3p constructs, respectively, have shown promising results (76, 77). Intrahippocampal miR-342 inhibition was shown to reduce β-amyloid plaques and ameliorate learning and memory in 3xTg-AD mice (76), a widely used murine model of pathological or behavioral abnormalities of AD, while suppression of miR-342 improved the expression of glutamate transporter, promoted dopaminergic neuron proliferation and suppressed apoptosis through the Wnt signaling pathway in mice with PD (77). Due to the interconnectivity and overlap of many neurocircuits and mechanisms between neurodegenerative and psychiatric

diseases, particularly in terms of neuroinflammation and microglial morphological and functional changes, we suggest miR-342 as a potential candidate target mediating inflammation-related depression.

In conclusion, we show that stressful early-life events, combined with high-CORT stress responsiveness, potentiate the development of depression-like behaviors and neuro-immunological alterations in adulthood, particularly increased microglial activation, TNF-α and miR-342 expression levels in the hippocampus. The potential of miR-342 as a therapeutic target in inflammation-related depression should be further investigated.

Acknowledgments

Authors would like to thank Dr. Arne Seitz and Dr. Romain Guiet from BioImaging and Optics Platform (BIOP, EPFL) for their valuable help in performing microglia morphological analysis. This project has been supported by grants from the Swiss National Science Foundation (SNSF) [NCCR Synapsy: 51NF40-158776 and -185897] and ERA-NET (Biostress; SNSF No 31NE30_189061). JPB was supported by *FCT - Fundação para a Ciência e a Tecnologia*, through BiotechHealth PhD program fellowship (PD/BD/135490/2018). SM was supported by NCCR Synapsy grant. MM was supported by an internal grant from the Donders Centre for Medical Neurosciences of the Radboudumc, and a personal travel grant from FENS. The funding sources had no additional role in study design, in the collection, analysis and interpretation of data, in the writing of the report, or in the decision to submit the paper for publication.

Competing Interests

The authors declare that they have no competing interests.

References

1. Krishnan V, Nestler EJ. The molecular neurobiology of depression. Nature. 2008;455(7215):894-902.
2. Miller AH, Raison CL. The role of inflammation in depression: from evolutionary imperative to modern treatment target. Nat Rev Immunol. 2016;16(1):22-34.
3. Miller AH. Beyond depression: the expanding role of inflammation in psychiatric disorders. World Psychiatry. 2020;19(1):108-9.
4. O'Brien SM, Scully P, Fitzgerald P, Scott LV, Dinan TG. Plasma cytokine profiles in depressed patients who fail to respond to selective serotonin reuptake inhibitor therapy. Journal of psychiatric research. 2007;41(3-4):326-31.
5. Fitzgerald P, O'Brien SM, Scully P, Rijkers K, Scott LV, Dinan TG. Cutaneous glucocorticoid receptor sensitivity and pro-inflammatory cytokine levels in antidepressant-resistant depression. Psychological medicine. 2006;36(1):37-43.
6. Harrison NA, Brydon L, Walker C, Gray MA, Steptoe A, Critchley HD. Inflammation causes mood changes through alterations in subgenual cingulate activity and mesolimbic connectivity. Biological psychiatry. 2009;66(5):407-14.
7. Lanquillon S, Krieg JC, Bening-Abu-Shach U, Vedder H. Cytokine production and treatment response in major depressive disorder. Neuropsychopharmacology : official publication of the American College of Neuropsychopharmacology. 2000;22(4):370-9.
8. Sluzewska A, Sobieska M, Rybakowski JK. Changes in acute-phase proteins during lithium potentiation of antidepressants in refractory depression. Neuropsychobiology. 1997;35(3):123-7.
9. Brás JP, Pinto S, Almeida MI, Prata J, von Doellinger O, Coelho R, et al. Peripheral Biomarkers of Inflammation in Depression: Evidence from Animal Models and Clinical Studies. In: Kobeissy FH, editor. Psychiatric Disorders: Methods and Protocols: Springer; 2019. p. 467-92.
10. Dheen ST, Kaur C, Ling EA. Microglial activation and its implications in the brain diseases. Current medicinal chemistry. 2007;14(11):1189-97.
11. Yirmiya R, Rimmerman N, Reshef R. Depression as a microglial disease. Trends in neurosciences. 2015;38(10):637-58.
12. Bezzi P, Domercq M, Brambilla L, Galli R, Schols D, De Clercq E, et al. CXCR4-activated astrocyte glutamate release via TNFalpha: amplification by microglia triggers neurotoxicity. Nat Neurosci. 2001;4(7):702-10.
13. Takeuchi H, Jin S, Wang J, Zhang G, Kawanokuchi J, Kuno R, et al. Tumor necrosis factor-alpha induces neurotoxicity via glutamate release from hemichannels of activated microglia in an autocrine manner. The Journal of biological chemistry. 2006;281(30):21362-8.
14. Block ML, Zecca L, Hong JS. Microglia-mediated neurotoxicity: uncovering the molecular mechanisms. Nature reviews Neuroscience. 2007;8.
15. Kuno R, Wang J, Kawanokuchi J, Takeuchi H, Mizuno T, Suzumura A. Autocrine activation of microglia by tumor necrosis factor-alpha. J Neuroimmunol. 2005;162(1-2):89-96.

16. Remus JL, Dantzer R. Inflammation Models of Depression in Rodents: Relevance to Psychotropic Drug Discovery. The international journal of neuropsychopharmacology. 2016;19(9).
17. Lasselin J, Schedlowski M, Karshikoff B, Engler H, Lekander M, Konsman JP. Comparison of bacterial lipopolysaccharide-induced sickness behavior in rodents and humans: Relevance for symptoms of anxiety and depression. Neuroscience & Biobehavioral Reviews. 2020;115:15-24.
18. Papilloud A, Guillot de Suduiraut I, Zanoletti O, Grosse J, Sandi C. Peripubertal stress increases play fighting at adolescence and modulates nucleus accumbens CB1 receptor expression and mitochondrial function in the amygdala. Translational psychiatry. 2018;8(1):156.
19. Walker SE, Zanoletti O, Guillot de Suduiraut I, Sandi C. Constitutive differences in glucocorticoid responsiveness to stress are related to variation in aggression and anxiety-related behaviors. Psychoneuroendocrinology. 2017;84:1-10.
20. Hohmann CF, Odebode G, Naidu L, Koban M. Early Life Stress Alters Adult Inflammatory Responses in a Mouse Model for Depression. Ann Psychiatry Ment Health. 2017;5(2):1095.
21. Miller AH. Inflammation Versus Glucocorticoids as Purveyors of Pathology during Stress: Have We Reached the Tipping Point? Biological psychiatry. 2008;64(4):263-5.
22. Heim C, Binder EB. Current research trends in early life stress and depression: review of human studies on sensitive periods, gene-environment interactions, and epigenetics. Experimental neurology. 2012;233(1):102-11.
23. Negele A, Kaufhold J, Kallenbach L, Leuzinger-Bohleber M. Childhood Trauma and Its Relation to Chronic Depression in Adulthood. Depress Res Treat. 2015;2015:650804-.
24. Marquez C, Poirier GL, Cordero MI, Larsen MH, Groner A, Marquis J, et al. Peripuberty stress leads to abnormal aggression, altered amygdala and orbitofrontal reactivity and increased prefrontal MAOA gene expression. Translational psychiatry. 2013;3:e216.
25. Reader BF, Jarrett BL, McKim DB, Wohleb ES, Godbout JP, Sheridan JF. Peripheral and Central Effects of Repeated Social Defeat Stress: Monocyte Trafficking, Microglial Activation, and Anxiety. Neuroscience. 2015;289:429-42.
26. Ulrich-Lai YM, Herman JP. Neural regulation of endocrine and autonomic stress responses. Nature Reviews Neuroscience. 2009;10(6):397-409.
27. Sorrells SF, Sapolsky RM. An inflammatory review of glucocorticoid actions in the CNS. Brain, behavior, and immunity. 2007;21(3):259-72.
28. Iob E, Kirschbaum C, Steptoe A. Persistent depressive symptoms, HPA-axis hyperactivity, and inflammation: the role of cognitive-affective and somatic symptoms. Molecular psychiatry. 2020;25(5):1130-40.
29. Silverman MN, Sternberg EM. Glucocorticoid regulation of inflammation and its functional correlates: from HPA axis to glucocorticoid receptor dysfunction. Annals of the New York Academy of Sciences. 2012;1261:55-63.
30. Sorrells SF, Caso JR, Munhoz CD, Sapolsky RM. The Stressed CNS: When Glucocorticoids Aggravate Inflammation. Neuron. 2009;64(1):33-9.
31. Almeida MI, Reis RM, Calin GA. MicroRNA history: discovery, recent applications, and next frontiers. Mutation research. 2011;717(1-2):1-8.
32. Wakabayashi T, Hidaka R, Fujimaki S, Asashima M, Kuwabara T. MicroRNAs and epigenetics in adult neurogenesis. Advances in genetics. 2014;86:27-44.

33. Issler O, Haramati S, Paul ED, Maeno H, Navon I, Zwang R, et al. MicroRNA 135 is essential for chronic stress resiliency, antidepressant efficacy, and intact serotonergic activity. Neuron. 2014;83(2):344-60.
34. Brites D, Fernandes A. Neuroinflammation and Depression: Microglia Activation, Extracellular Microvesicles and microRNA Dysregulation. Front Cell Neurosci. 2015;9:476.
35. Brás JP, Bravo J, Freitas J, Barbosa MA, Santos SG, Summavielle T, et al. TNF-alpha-induced microglia activation requires miR-342: impact on NF-kB signaling and neurotoxicity. Cell Death & Disease. 2020;11(6):415.
36. Larsen MH, Mikkelsen JD, Hay-Schmidt A, Sandi C. Regulation of brain-derived neurotrophic factor (BDNF) in the chronic unpredictable stress rat model and the effects of chronic antidepressant treatment. Journal of psychiatric research. 2010;44(13):808-16.
37. Bustin SA, Benes V, Garson JA, Hellemans J, Huggett J, Kubista M, et al. The MIQE guidelines: minimum information for publication of quantitative real-time PCR experiments. Clinical chemistry. 2009;55(4):611-22.
38. Schindelin J, Arganda-Carreras I, Frise E, Kaynig V, Longair M, Pietzsch T, et al. Fiji: an open-source platform for biological-image analysis. Nature Methods. 2012;9(7):676-82.
39. Ollion J, Cochennec J, Loll F, Escudé C, Boudier T. TANGO: a generic tool for high-throughput 3D image analysis for studying nuclear organization. Bioinformatics. 2013;29(14):1840-1.
40. Walker SE, Sandi C. Long-term programing of psychopathology-like behaviors in male rats by peripubertal stress depends on individual's glucocorticoid responsiveness to stress. Stress (Amsterdam, Netherlands). 2018;21(5):433-42.
41. Inostroza M, Cid E, Menendez de la Prida L, Sandi C. Different Emotional Disturbances in Two Experimental Models of Temporal Lobe Epilepsy in Rats. PloS one. 2012;7(6):e38959.
42. Davis BM, Salinas-Navarro M, Cordeiro MF, Moons L, De Groef L. Characterizing microglia activation: a spatial statistics approach to maximize information extraction. Scientific Reports. 2017;7(1):1576.
43. Osimo EF, Pillinger T, Rodriguez IM, Khandaker GM, Pariante CM, Howes OD. Inflammatory markers in depression: A meta-analysis of mean differences and variability in 5,166 patients and 5,083 controls. Brain, behavior, and immunity. 2020;87:901-9.
44. Dowlati Y, Herrmann N, Swardfager W, Liu H, Sham L, Reim EK, et al. A meta-analysis of cytokines in major depression. Biological psychiatry. 2010;67(5):446-57.
45. Hiles SA, Baker AL, de Malmanche T, Attia J. Interleukin-6, C-reactive protein and interleukin-10 after antidepressant treatment in people with depression: a meta-analysis. Psychological medicine. 2012;42(10):2015-26.
46. Sluzewska A, Rybakowski JK, Laciak M, Mackiewicz A, Sobieska M, Wiktorowicz K. Interleukin-6 serum levels in depressed patients before and after treatment with fluoxetine. Annals of the New York Academy of Sciences. 1995;762:474-6.
47. Jazayeri S, Keshavarz SA, Tehrani-Doost M, Djalali M, Hosseini M, Amini H, et al. Effects of eicosapentaenoic acid and fluoxetine on plasma cortisol, serum interleukin-1beta and interleukin-6 concentrations in patients with major depressive disorder. Psychiatry research. 2010;178(1):112-5.

48. Kubera M, Kenis G, Bosmans E, Kajta M, Basta-Kaim A, Scharpe S, et al. Stimulatory effect of antidepressants on the production of IL-6. International immunopharmacology. 2004;4(2):185-92.
49. Strawbridge R, Arnone D, Danese A, Papadopoulos A, Herane Vives A, Cleare AJ. Inflammation and clinical response to treatment in depression: A meta-analysis. European neuropsychopharmacology : the journal of the European College of Neuropsychopharmacology. 2015;25(10):1532-43.
50. Haroon E, Daguanno AW, Woolwine BJ, Goldsmith DR, Baer WM, Wommack EC, et al. Antidepressant treatment resistance is associated with increased inflammatory markers in patients with major depressive disorder. Psychoneuroendocrinology. 2018;95:43-9.
51. Bunea IM, Szentágotai-Tătar A, Miu AC. Early-life adversity and cortisol response to social stress: a meta-analysis. Translational psychiatry. 2017;7(12):1274.
52. Taylor SE. Mechanisms linking early life stress to adult health outcomes. Proceedings of the National Academy of Sciences. 2010;107(19):8507-12.
53. Juruena MF. Early-life stress and HPA axis trigger recurrent adulthood depression. Epilepsy & Behavior. 2014;38:148-59.
54. Johnson SA, Fournier NM, Kalynchuk LE. Effect of different doses of corticosterone on depression-like behavior and HPA axis responses to a novel stressor. Behavioural brain research. 2006;168(2):280-8.
55. Goodwill HL, Manzano-Nieves G, Gallo M, Lee H-I, Oyerinde E, Serre T, et al. Early life stress leads to sex differences in development of depressive-like outcomes in a mouse model. Neuropsychopharmacology : official publication of the American College of Neuropsychopharmacology. 2019;44(4):711-20.
56. Kappelmann N, Lewis G, Dantzer R, Jones PB, Khandaker GM. Antidepressant activity of anti-cytokine treatment: a systematic review and meta-analysis of clinical trials of chronic inflammatory conditions. Molecular psychiatry. 2018;23(2):335-43.
57. Raison CL, Rutherford RE, Woolwine BJ, et al. A randomized controlled trial of the tumor necrosis factor antagonist infliximab for treatment-resistant depression: The role of baseline inflammatory biomarkers. JAMA Psychiatry. 2013;70(1):31-41.
58. Loftus EV, Feagan BG, Colombel JF, Rubin DT, Wu EQ, Yu AP, et al. Effects of adalimumab maintenance therapy on health-related quality of life of patients with Crohn's disease: patient-reported outcomes of the CHARM trial. The American journal of gastroenterology. 2008;103(12):3132-41.
59. Menter A, Augustin M, Signorovitch J, Yu AP, Wu EQ, Gupta SR, et al. The effect of adalimumab on reducing depression symptoms in patients with moderate to severe psoriasis: a randomized clinical trial. Journal of the American Academy of Dermatology. 2010;62(5):812-8.
60. Tyring S, Gottlieb A, Papp K, Gordon K, Leonardi C, Wang A, et al. Etanercept and clinical outcomes, fatigue, and depression in psoriasis: double-blind placebo-controlled randomised phase III trial. Lancet (London, England). 2006;367(9504):29-35.
61. Tyring S, Bagel J, Lynde C, Klekotka P, Thompson EH, Gandra SR, et al. Patient-reported outcomes in moderate-to-severe plaque psoriasis with scalp involvement: results from a randomized, double-blind, placebo-controlled study of etanercept. Journal of the European Academy of Dermatology and Venereology : JEADV. 2013;27(1):125-8.

62. Golan H, Levav T, Mendelsohn A, Huleihel M. Involvement of tumor necrosis factor alpha in hippocampal development and function. Cerebral cortex (New York, NY : 1991). 2004;14(1):97-105.
63. Dantzer R, O'Connor JC, Freund GG, Johnson RW, Kelley KW. From inflammation to sickness and depression: when the immune system subjugates the brain. Nature reviews Neuroscience. 2008;9(1):46-56.
64. Olmos G, Llado J. Tumor necrosis factor alpha: a link between neuroinflammation and excitotoxicity. Mediators of inflammation. 2014;2014:12.
65. Gomez-Nicola D, Perry VH. Microglial Dynamics and Role in the Healthy and Diseased Brain: A Paradigm of Functional Plasticity. The Neuroscientist. 2014;21(2):169-84.
66. Tang Y, Le W. Differential Roles of M1 and M2 Microglia in Neurodegenerative Diseases. Molecular Neurobiology. 2016;53(2):1181-94.
67. Gong Y, Tong L, Yang R, Hu W, Xu X, Wang W, et al. Dynamic changes in hippocampal microglia contribute to depressive-like behavior induced by early social isolation. Neuropharmacology. 2018;135:223-33.
68. Pan Y, Chen XY, Zhang QY, Kong LD. Microglial NLRP3 inflammasome activation mediates IL-1β-related inflammation in prefrontal cortex of depressive rats. Brain, behavior, and immunity. 2014;41:90-100.
69. Catale C, Gironda S, Lo Iacono L, Carola V. Microglial Function in the Effects of Early-Life Stress on Brain and Behavioral Development. J Clin Med. 2020;9(2):468.
70. Calin GA, Dumitru CD, Shimizu M, Bichi R, Zupo S, Noch E, et al. Frequent deletions and down-regulation of micro-RNA genes miR15 and miR16 at 13q14 in chronic lymphocytic leukemia. Proceedings of the National Academy of Sciences. 2002;99(24):15524-9.
71. Almeida MI, Reis RM, Calin GA. Decoy activity through microRNAs: the therapeutic implications. Expert opinion on biological therapy. 2012;12(9):1153-9.
72. Xu J, Wang R, Liu Y, Wang W, Liu D, Jiang H, et al. Short- and long-term alterations of FKBP5-GR and specific microRNAs in the prefrontal cortex and hippocampus of male rats induced by adolescent stress contribute to depression susceptibility. Psychoneuroendocrinology. 2019;101:204-15.
73. Liu CP, Zhong M, Sun JX, He J, Gao Y, Qin FX. miR-146a reduces depressive behavior by inhibiting microglial activation. Molecular medicine reports. 2021;23(6).
74. Chen L, Dong R, Lu Y, Zhou Y, Li K, Zhang Z, et al. MicroRNA-146a protects against cognitive decline induced by surgical trauma by suppressing hippocampal neuroinflammation in mice. Brain, behavior, and immunity. 2019;78:188-201.
75. Tzanoulinou S, Gantelet E, Sandi C, Márquez C. Programming effects of peripubertal stress on spatial learning. Neurobiology of Stress. 2020;13:100282.
76. Fu Y, Hu X, Zheng C, Sun G, Xu J, Luo S, et al. Intrahippocampal miR-342-3p inhibition reduces β-amyloid plaques and ameliorates learning and memory in Alzheimer's disease. Metabolic brain disease. 2019;34(5):1355-63.
77. Wu DM, Wang S, Wen X, Han XR, Wang YJ, Shen M, et al. Suppression of microRNA-342-3p increases glutamate transporters and prevents dopaminergic neuron loss through activating the Wnt signaling pathway via p21-activated kinase 1 in mice with Parkinson's disease. Journal of cellular physiology. 2019;234(6):9033-44.

Supplementary Information

Stress-induced depressive-like behavior in male rats is associated with microglial activation and inflammation dysregulation in the hippocampus in adulthood

João Paulo Brás[1,2,3], Isabelle Guillot de Suduiraut[3], Olivia Zanoletti[3], Silvia Monari[3], Mandy Meijer[3,4], Jocelyn Grosse[3], Mário Adolfo Barbosa[1,2], Susana Gomes Santos[1], Carmen Sandi[3], Maria Inês Almeida[1,2,#]

Affiliations

[1] Instituto de Investigação e Inovação em Saúde/Instituto de Engenharia Biomédica (i3S/INEB), University of Porto (UP), Rua Alfredo Allen 208, 4200-135 Porto, Portugal

[2] Instituto de Ciências Biomédicas Abel Salazar (ICBAS), University of Porto (UP), Rua de Jorge Viterbo Ferreira 228, 4050-313 Porto, Portugal

[3] Brain Mind Institute, École Polytechnique Fédérale de Lausanne (EPFL), Station 19, CH-1015 Lausanne, Switzerland

[4] Department of Human Genetics, Donders Institute for Brain, Cognition and Behaviour, Radboud University Medical Center, Nijmegen, Netherlands.

Corresponding author: ines.almeida@i3s.up.pt

Table S1 - Oligonucleotides sequences for RT-qPCR. Oligonucleotides used to amplify rat mRNAs encoding inflammatory markers and reference genes, based on GenBank sequences. Abbreviations: Iba1, ionized calcium-binding adapter molecule 1; Il1b, interleukin 1 beta; Il6, interleukin 6; Tnf, tumour necrosis factor; Gapdh, glyceraldehyde 3-phosphate dehydrogenase; B-actin, beta-actin.

Gene	Accession Number	Forward (5'-3')	Reverse (5'-3')
Rat *Iba1*	NM_017196	GCCTCATCGTCATCTCCCCA	AGGAAGTGCTTGTTGATCCCA
Rat *Il1b*	NM_031512	CACCTTCTTTTCCTTCATCTTTG	GTCGTTGCTTGTCTCTCCTTGTA
Rat *Il6*	NM_012589	CATATGTTCTCAGGGAGATCTTGGA	CAGTGCATCATCGCTGTTCA
Rat *Tnf*	NM_012675	CCCAGACCCTCACACTCAGAT	TTGTCCCTTGAAGAGAACCTG
Rat *Gapdh*	NM_017008	CCCCCAATGTATCCGTTGTG	TAGCCCAGGATGCCCTTTAGT
Rat *B-actin*	NM_031144	AGAAGAGCTATGAGCTGCCTGACG	TACTTGCGCTCAGGAGGAGCAATG

Table S2 - Expression levels of inflammatory markers across different brain regions in adulthood. The mRNA expression levels of IL-1β, IL-6, TNF-α and IBA-1 in the mPFC, NAc, Amg and HPC were evaluated by RT-qPCR using GAPDH and β-actin as internal controls. Relative expression levels were calculated using the quantification cycle (Cq) method, according to MIQE guidelines, and results are presented as mean ± SEM. N: N-CSR = 18 (9 CTR and 9 PPS); H-CSR = 24 (12 CTR and 12 PPS); 2-way ANOVA test was performed to evaluate the impact of different CSRs and stress exposure in the expression levels of the inflammatory markers. Differences between corresponding CTR and PPS groups were evaluated by Sidak's post-hoc multiple comparisons. Where a significant difference was found between CTR and PPS groups, gene names are shown in bold (n.s.: non-significant; *p < 0.05; **p<0.01; ***p<0.001).

Brain Region	Gene	N-CSR				H-CSR				2-way ANOVA			
		CTR (n=9)		PPS (n=9)		CTR (n=12)		PPS (n=12)		Row factor (N-CSRvsH-CSR)		Post-hoc Comparison	
		mean	SEM	mean	SEM	mean	SEM	mean	SEM	F	p-value	N-CSR: CTRvsPPS	H-CSR: CTRvsPPS
mPFC	*Il1b*	0.000046	0.000003	0.000053	0.000005	0.000075	0.000009	0.000082	0.000007	17.12	***	n.s.	n.s.
	Il6	0.000074	0.000004	0.000065	0.000004	0.000112	0.000005	0.000100	0.000007	42.32	***	n.s.	n.s.
	Tnf	0.000213	0.000015	0.000224	0.000020	0.000182	0.000011	0.000192	0.000020	3.56	n.s.	n.s.	n.s.
	Iba1	0.014040	0.000453	0.014730	0.000594	0.023110	0.001216	0.021510	0.000980	67.76	***	n.s.	n.s.
NAc	*Il1b*	0.000240	0.000050	0.000560	0.000168	0.000727	0.000139	0.000930	0.000242	5.51	*	n.s.	n.s.
	Il6	0.025950	0.003921	0.031440	0.006846	0.040660	0.005745	0.053930	0.004819	11.40	**	n.s.	n.s.
	Tnf	0.006513	0.000943	0.008705	0.001661	0.009014	0.001989	0.016230	0.002476	5.96	*	n.s.	*
	Iba1	0.037230	0.006375	0.044400	0.006552	0.040000	0.004609	0.037750	0.004921	0.12	n.s.	n.s.	n.s.
Amg	*Il1b*	0.000297	0.000098	0.000142	0.000036	0.000137	0.000031	0.000181	0.000039	1.28	n.s.	n.s.	n.s.
	Il6	0.037020	0.004712	0.028200	0.005969	0.042220	0.006793	0.040810	0.007785	1.72	n.s.	n.s.	n.s.
	Tnf	0.012050	0.001540	0.009273	0.001821	0.014230	0.002587	0.012430	0.001346	1.92	n.s.	n.s.	n.s.
	Iba1	0.038760	0.003382	0.046600	0.002575	0.041680	0.003269	0.038450	0.002361	0.79	n.s.	n.s.	n.s.
HPC	*Il1b*	0.000545	0.000120	0.001020	0.000345	0.000405	0.000133	0.000549	0.000184	2.16	n.s.	n.s.	n.s.
	Il6	0.005385	0.001359	0.005464	0.000974	0.004722	0.000513	0.007372	0.000862	0.45	n.s.	n.s.	n.s.
	Tnf	0.000579	0.000108	0.001936	0.000475	0.001082	0.000155	0.001994	0.000362	1.12	n.s.	*	*
	Iba1	0.026440	0.004994	0.029170	0.006052	0.017010	0.002968	0.049720	0.009336	0.71	n.s.	n.s.	**

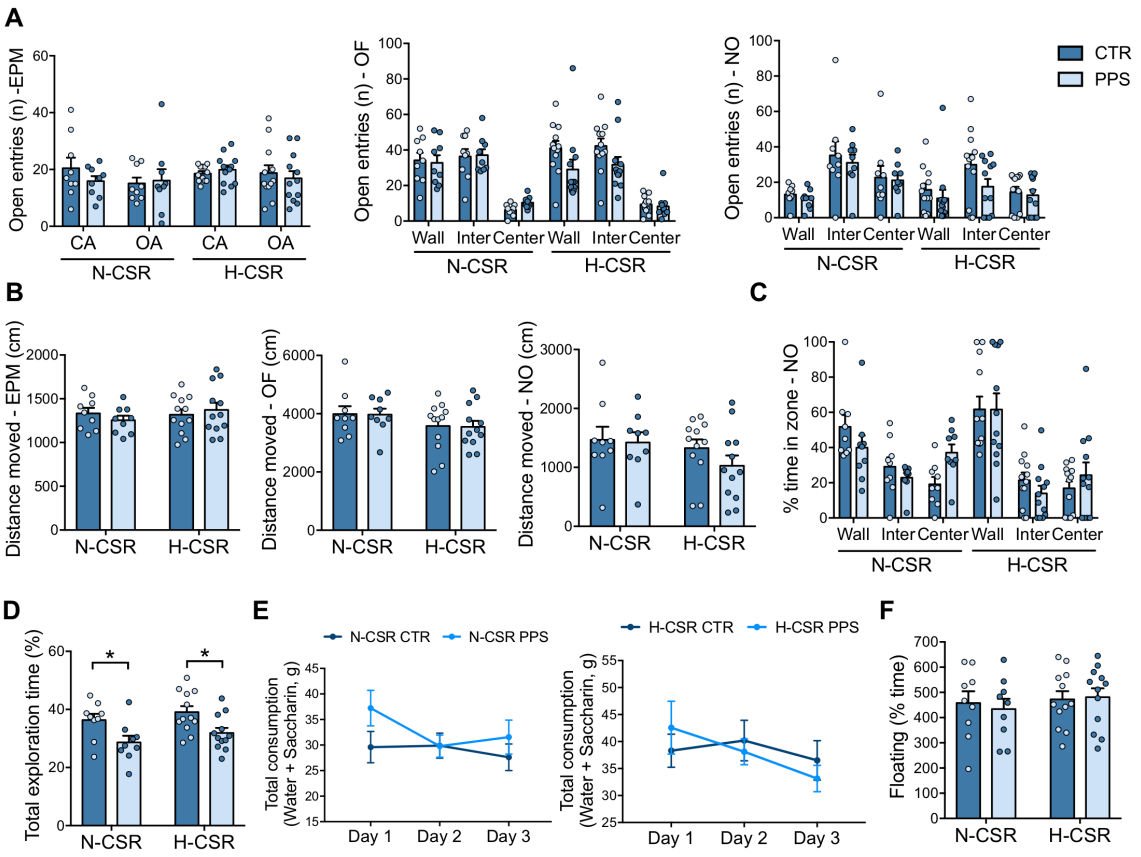

Figure S1 – Supplementary behavioral results. Number of open entries in zone (A) and total distance moved (B) in the EPM and OF/NO were calculated using EthoVision 11. After the OF test, a NO was introduced in the center and the behavior observed for extra 5 min. % time spent in zone and was calculated using EthoVision 11 (C). In the SocPT, total exploration time was scored using Observer X11 (D). In the SacPT, total consumption (water + saccharin) was calculated (E). In the FST, two trials were performed and recorded. The graph represents the % time the animal spent floating in the first trial, lasting 15 min (F). N: N-CSR = 18 (9 CTR and 9 PPS); H-CSR = 24 (12 CTR and 12 PPS). Results are expressed as mean ± SEM. 2-way ANOVA followed by Sidak's multiple comparisons, *p < 0.05. CA - closed arms, OA - open arms.

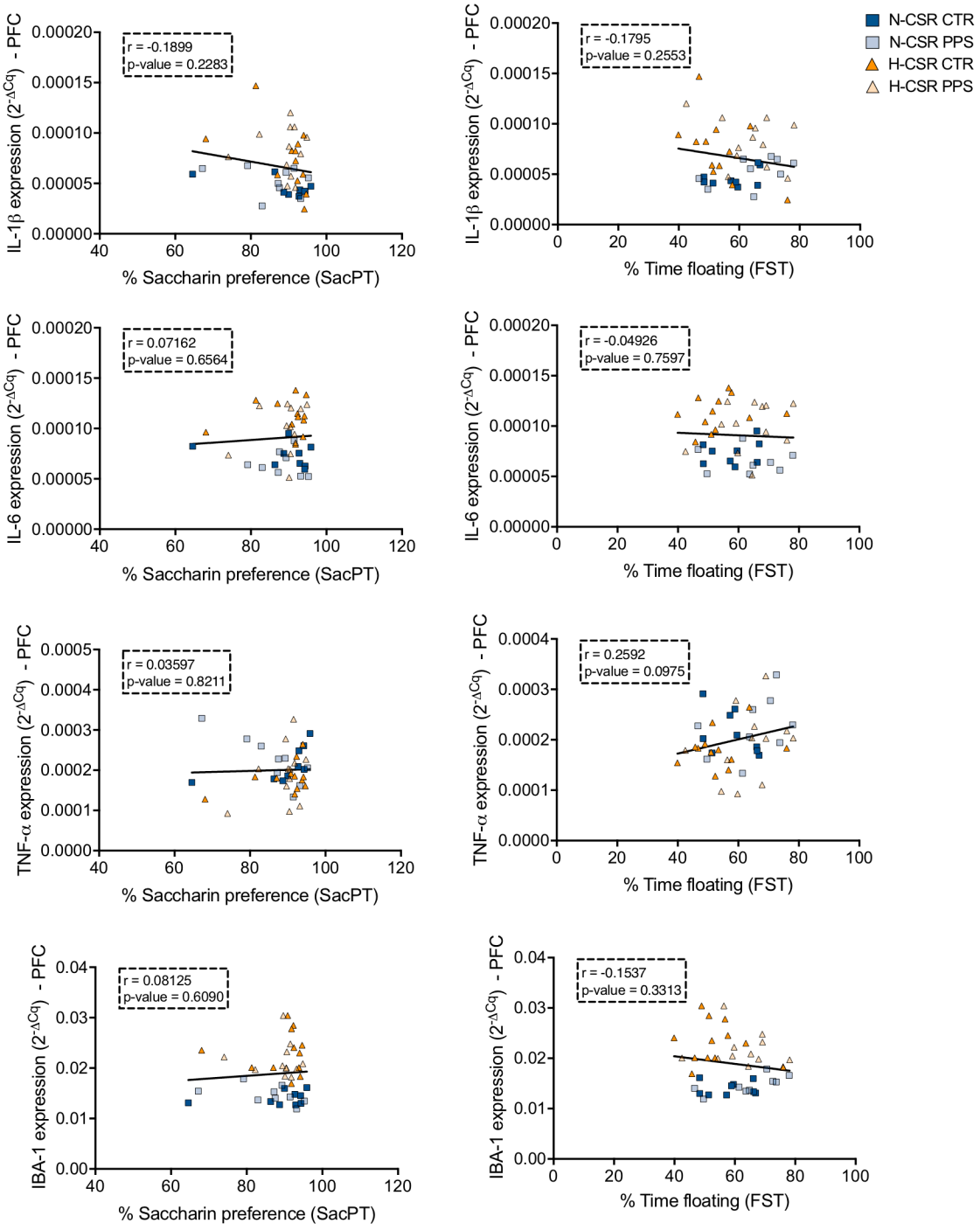

Figure S2 – Correlations between the expression levels of inflammatory markers in the mPFC and depressive-like behaviors. Pearson correlations were performed by comparing mRNA expression levels of IL-1β, IL-6, TNF-α and IBA-1 in the medial pre-frontal cortex (mPFC) and % saccharin preference (SacPT) or % time floating (FST). Correlations were performed considering all animals (N=42). Coefficient r and p-value for each correlation are presented in a box. Statistically significant correlations are highlighted in green ($p<0.05$).

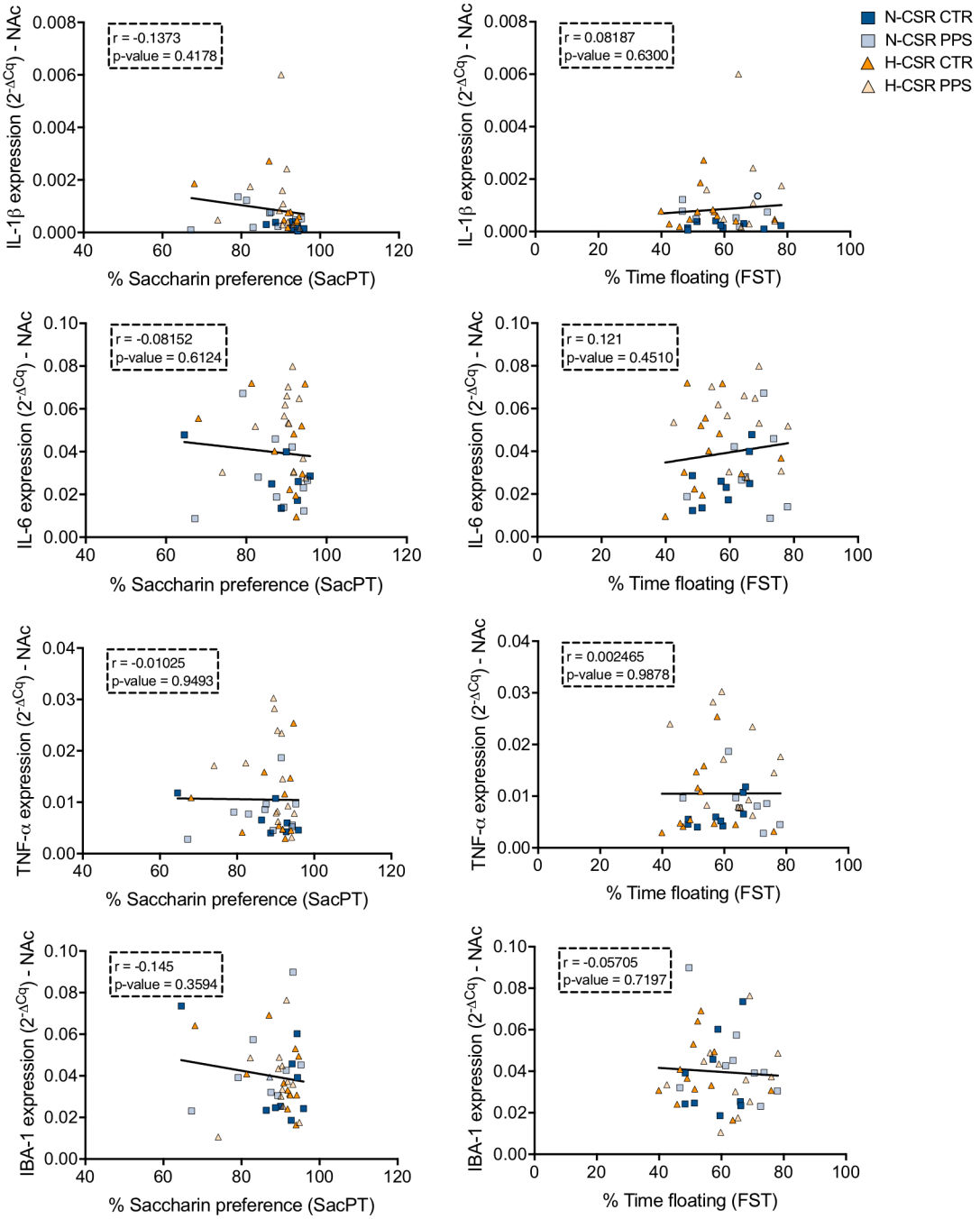

Figure S3 – Correlations between the expression levels of inflammatory markers in the NAc and depressive-like behaviors. Pearson correlations were performed by comparing mRNA expression levels of IL-1β, IL-6, TNF-α and IBA-1 in the nucleus accumbens (NAc) and % saccharin preference (SacPT) or % time floating (FST). Correlations were performed considering all animals (N=42). Coefficient r and p-value for each correlation are presented in a box. Statistically significant correlations are highlighted in green ($p<0.05$).

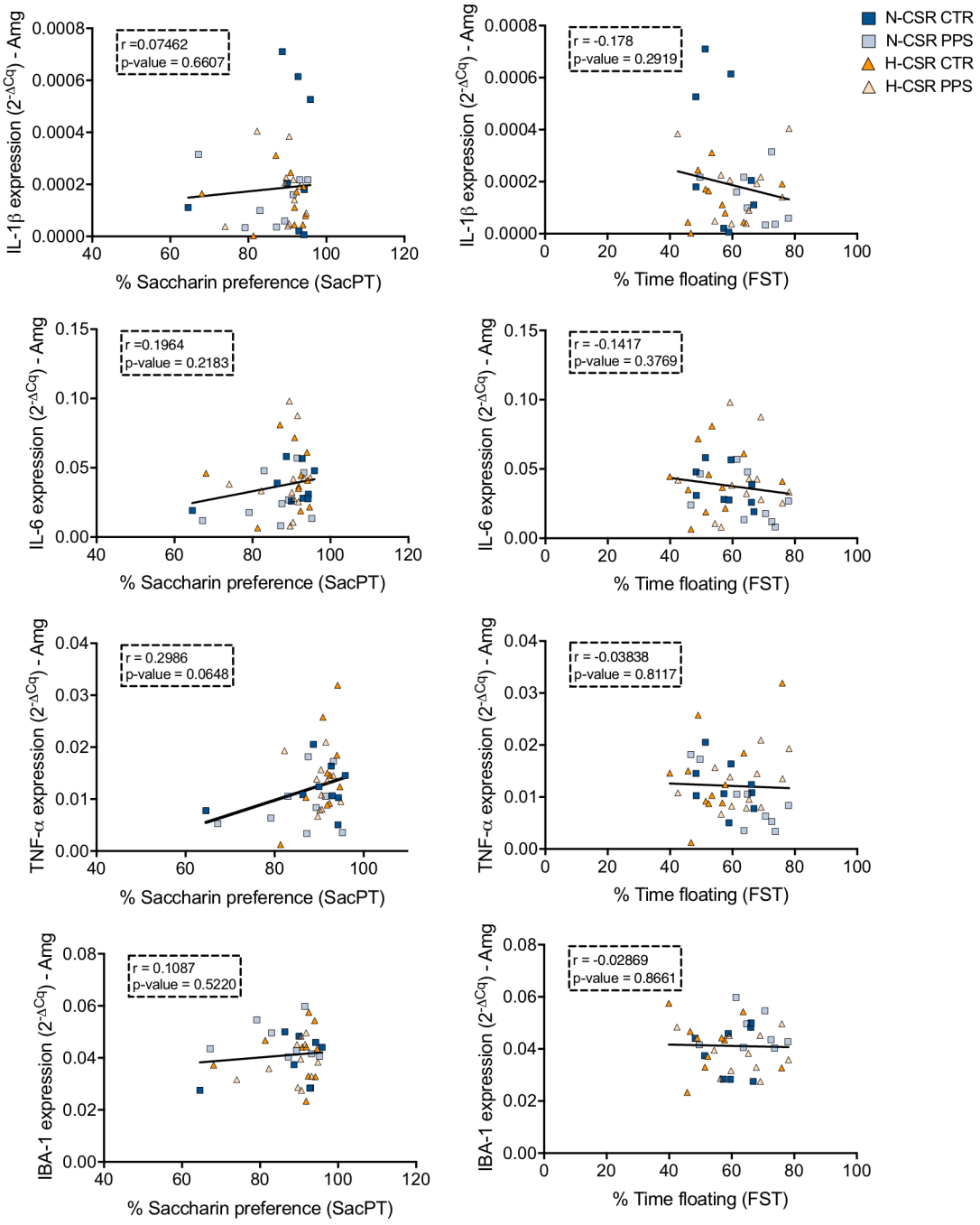

Figure S4 – Correlations between the expression levels of inflammatory markers in the Amg and depressive-like behaviors. Pearson correlations were performed by comparing mRNA expression levels of IL-1β, IL-6, TNF-α and IBA-1 in the amygdala (Amg) and % saccharin preference (SacPT) or % time floating (FST). Correlations were performed considering all animals (N=42). Coefficient r and p-value for each correlation are presented in a box. Statistically significant correlations are highlighted in green ($p<0.05$).

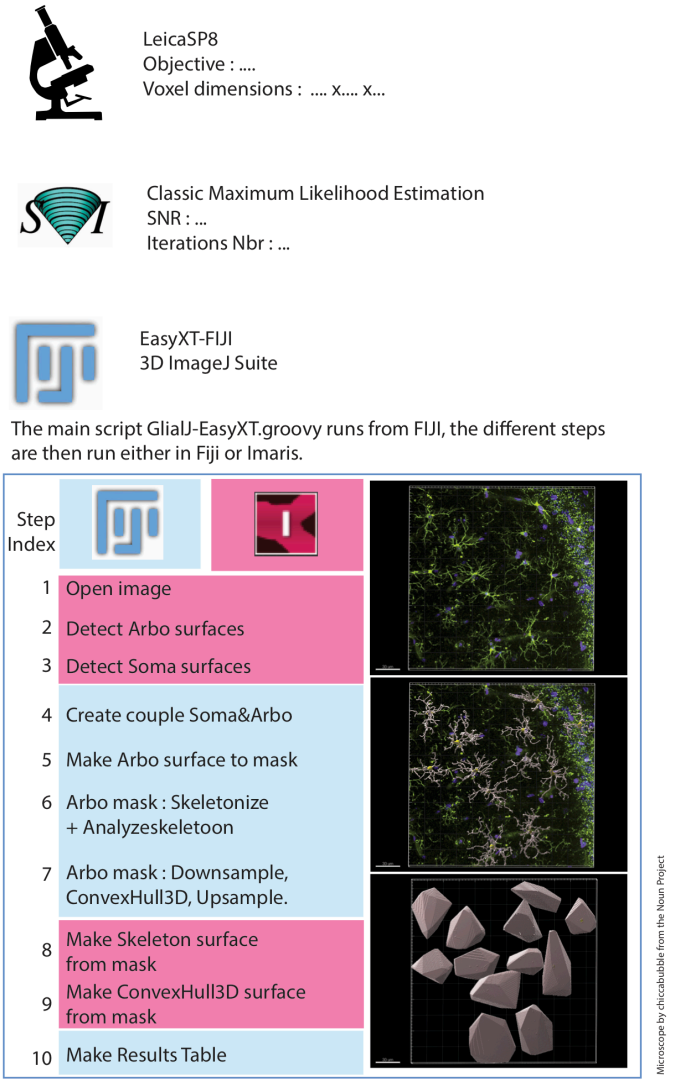

Figure S5 – Microglia 3D morphological analysis: step-by-step. Images were acquired using Leica SP8 with a 40x glycerin immersion objective. The pixel size was set to 0.230 microns. The acquired images were deconvolved using SVI Huygens Professional called via Huygens Remote Manager v3.7, using the "Classic Maximum Likelihood Estimation" algorithm. The analysis of the deconvolved images was performed with Fiji and Imaris using the EasyXT-Fiji plugin via a custom groovy script. Imaris surfaces were created to segment the arborization of the cells and for their soma. Next, cells were created by linking the soma to its corresponding arborization, based on the nearest centers of mass (Step Index 1-3). Next, for each cell, the mask of the arborization was sent to Fiji: 1) skeletonized and analyzed (average and maximum branch length, number of branches), and 2) down sampled, in order to calculate its 3D ConvexHull, which was then upscaled back to the original size (Step Index 4-7). Finally, the masks of the Skeleton and of the 3D ConvexHull were sent back to the Imaris Scene (Step Index 8 and 9) and a results file was created with volumes and calculated ratios (Step Index 10).

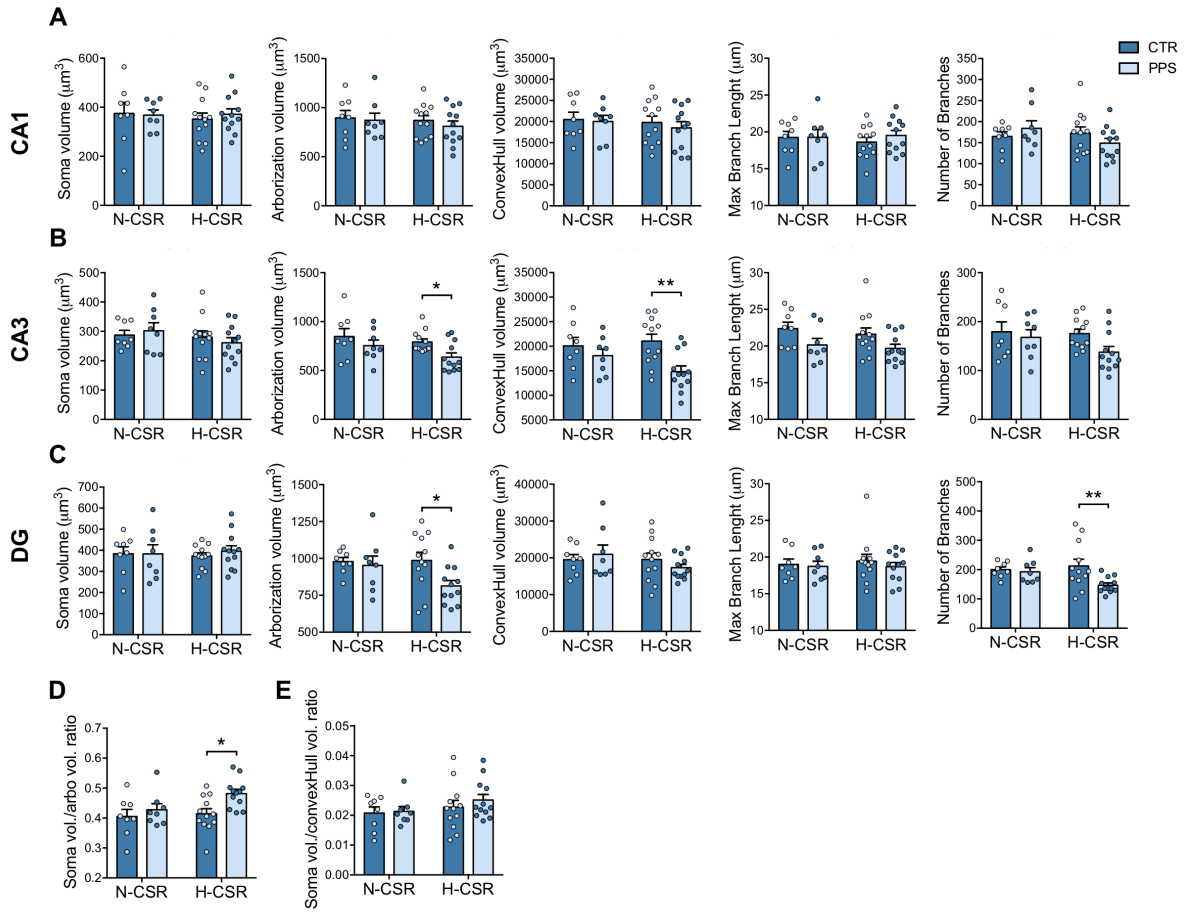

Figure S6 - Quantitative analysis of microglial morphology in CA1, CA3 and DG hippocampal subregions. Results represent microglial morphological parameters quantified in the CA1 (A), CA3 (B) and DG (C) subregions. On average, more than 20 cells per animal were analysed in terms of soma volume, arborization volume, convexHull volume, max branch length and number of branches. Graph (D) show the ratio between soma volume and arborization volume and (E) the ratio between soma volume and ConvexHull volume, considering the average values of the 3 fields (CA1, CA3 and DG). Each dot represents an animal (N: N-CSR = 18 (9 CTR and 9 PPS); H-CSR = 24 (12 CTR and 12 PPS). Results are expressed as mean ± SEM. 2-way ANOVA followed by Sidak's multiple comparisons, *p < 0.05.